Project #: DJO - 0107

WIND POWER FROM KITES

A Major Qualifying Project Report
Submitted to the Faculty
of the

WORCESTER POLYTECHNIC INSTITUTE

in partial fulfillment of the requirements for the
Degree of Bachelor of Science
In Aerospace Engineering

SUBMITTED BY:

Michael R. Blouin Jr.
mikeblou@wpi.edu

Benjamin E. Isabella
isabella@wpi.edu

Joshua E. Rodden
jrodden@wpi.edu

Date: April 27th, 2007

Professor David Olinger, Project Advisor

Abstract

The goal of this project was to study the feasibility of using tethered kites to generate power from the wind. Generating electricity using kites instead of wind turbines may have certain advantages, particularly for developing nations. These include generating power at low cost while eliminating certain environmental problems associated with wind turbines. Another advantage is that kites can fly at greater heights than wind turbines can operate. Since wind speed increases with height, and available power is proportional to wind speed cubed, the wind power potential is larger for kites. A literature review was conducted of previous studies of kite power systems. A mechanism was designed to convert the oscillating tether tension caused by the vertical motion of a kite into rotary shaft motion to drive a generator. The mechanism is based on a rocking, balanced beam of 5 meter length attached to a power train and Sprag clutch. The design uses a commercially available sport kite which is 10 meters squared in size. A previously developed MATLAB code was used to model the final system design, and power outputs comparable to small wind turbines were predicted.

Acknowledgements

The Wind Power from Kites group would like to thank:

Professor David J. Olinger
For his guidance, leadership, encouragement, and enthusiasm on this project from the beginning of development.

Dr. J. S. Goela
For originally conceiving the concept of wind power from kites as well as acting as technical consultant throughout the duration of the development of this project.

Andrew Ghezzi, owner of Powerline Sports in Seabrook, NH
For his insight into kite dynamics and the sport of kite boarding as well as the instruction for proper operation of our kite.

Professor Gatsonis, Professor Blandino, Professor Demetriou, and Professor Hussein
For constructive criticism and guidance presented during weekly AE MQP presentations.

Fellow Aerospace Engineering Students
For constructive criticism and encouragement during weekly AE MQP presentations.

Dale Perkins
For allowing the use of Overlook Farms as the primary test site for the kite power demonstrator.

The Staff of the WPI Machine Shops
For assistance in dealing with minor issues with part tolerances in a timely fashion.

Col. Ken Stafford
For introducing us to the idea of using a sprag clutch in the final mechanism design.

Table of Contents

Table of Figures

List of Tables

1. Introduction

There are several sources of renewable energy currently in use today including bio-fuels, solar energy, hydrogen fuel cells, and wind power. The focus of this project will be on wind power and its potential use in a developing nation. Wind power production provides several significant benefits when being considered for integration into the infrastructure of a developing nation or a rural area. Wind turbines are generally used to generate power from the wind. Wind power systems, such as wind turbines, do not need long transmission lines and therefore can create and distribute electrical power outside the electrical grid.

Though it is apparent that there are significant advantages to employing wind power systems in developing nations, there are a number of significant disadvantages to the current primary source of wind energy, the wind turbine. When considering use in a developing nation, a wind turbine is a very expensive commodity. Wind turbines include several components; a set of fan blades, a large tower, a power conversion system, and a battery storage unit. Another significant drawback for the wind turbine is the impact that it has on the environment. Even though the wind turbine eliminates the greenhouse emissions typical of fossil fuel systems, wind turbines produce a considerable amount of noise pollution, visual pollution, and are believed to be a significant cause of bird deaths.

The concept of a kite powered wind energy system can eliminate these disadvantages while retaining the advantages of a wind power system. This proposed system would convert wind power into a usable form of energy, either electrical or mechanical. For the production of electrical energy, the kite system will employ a system to convert the up and down linear motion of a kite tether, as the angle of attack is

changed, into a rotary motion of a shaft. Connection of the shaft to a generator will produce an electrical current that can be stored in batteries.

A kite driven energy system has the potential to have significantly lower costs than a wind turbine as there is no need for the large tower that a wind turbine requires. Without the large turning blades of the wind turbine the noise pollution and bird hazard concerns are eliminated. The concern with visual pollution is also eliminated as kite systems would not negatively impact attractive natural landscapes.

The kite powered system can be implemented in areas with larger variations in wind velocity as the kite has the ability to reach much greater altitudes. The advantage of reaching much greater altitudes is that at higher altitudes the wind velocity is higher and more constant with less gusting. A generally recognized 'rule of thumb' is that wind speed increases to the 1/7th power of the change in height above ground. Figure 1 is a comparison between the potential power output and the wind velocities available to a 10m^2 kite and wind turbine. Power increases proportionally with the cube of the wind velocity, $P \alpha V^3$, and therefore increases in altitude result in greater increases in power output potential.

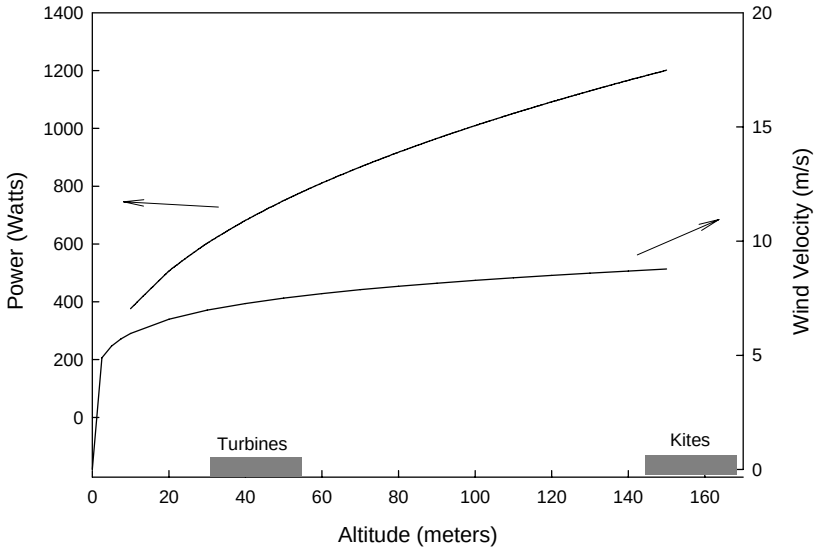

Figure 1 - Power output and wind velocity for turbine or kite with A = 10 m2 area.

1.1 Previous Research

Fossil fuel exhaustion concerns during the past few decades have given rise to renewed interest in renewable energy sources. Therefore, there has been an increasing amount of research done into different types of renewable energy sources. Wind power is believed to be a beneficial form of renewable energy. With the goal of decreasing the costs of this already cheap form of energy, scientists and enthusiasts alike have been studying the feasibility of using kites to harness wind power and convert it into a useful form of mechanical or electrical energy.

There have been a large number of concepts and designs created for systems intended to convert wind power into electrical energy as well. At this time it seems as though the majority of systems that have been designed for the production of electrical energy have been extremely complex and large in size. One example of a very large kite power system is the “KiteGen”, as seen in Figure 2. It is believed that this system designed in Italy has the potential of replacing a nuclear power plant. The KiteGen

resembles a very large merry-go-round with stacked kites attached to the outer rim so as to turn a large platform, producing the electrical energy. (sequoiaonline.com, 2006)

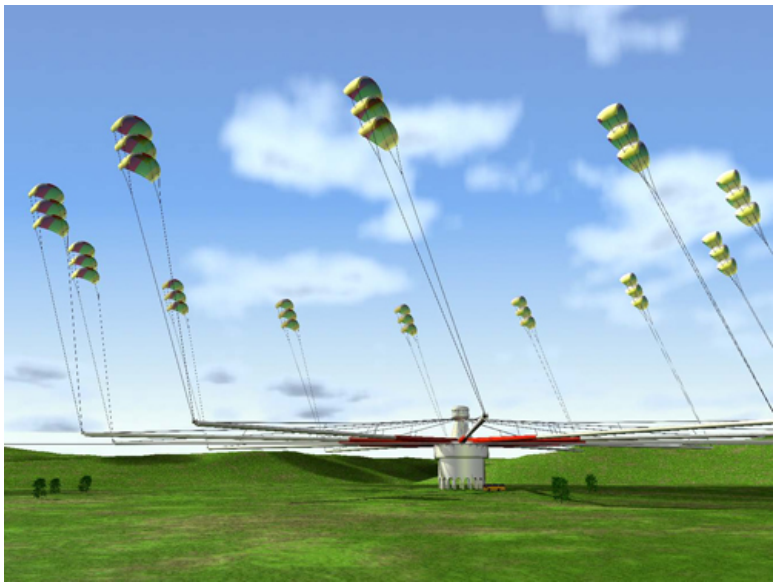

(http://www.wired.com/science/discoveries/news/2006/10/71908)

Figure 2 - KiteGen concept

Lang (2005) compares and studies the feasibility of several different concepts for systems designed to convert wind power into electrical energy using kites. Lang uses a detailed decision matrix to compare six different concepts for system designs and ultimately determined what he objectively believed to be the most feasible options. Of the six concepts compared, the two top scoring concepts were the "KiwiGen", and the "Reel." The KiwiGen is the same concept as the KiteGen described above. The Reel, shown in Figure 3, is a concept utilizing a series of mechanical and electrical components to harvest energy from the kite as it is pulled out and wound back in. The kite in the Reel concept is pulled out when it is at a high angle of attack until the angle of attack is mechanically changed and the kite is pulled in by another mechanical component. The

resultant energy is the energy gained from the turning gears as the kite is pulled out minus the mechanical energy required to reel the kite back in to restart the cycle.

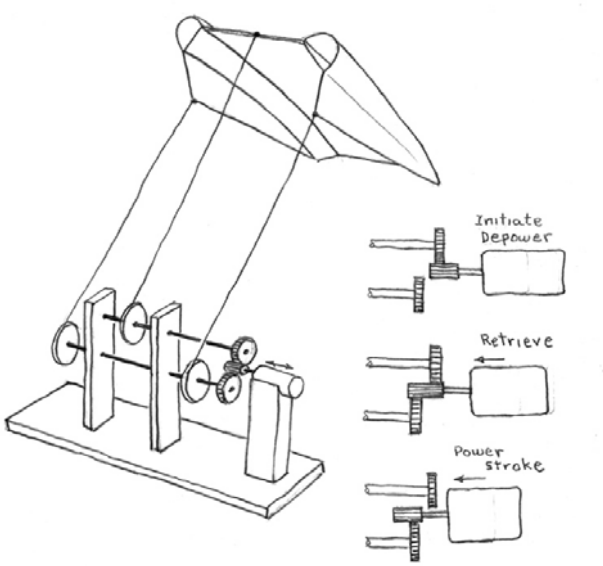

Figure 3 - David Lang's Reel Concept

Above are examples of relatively recent developments in wind power harnessing to produce a usable form of energy, but there were numerous studies done in the 1970's and 1980's as well. Loyd (1979) analyzed the power potential of large area kites in crosswind conditions. This study developed equations of kite motion when interacting in the crosswind direction with the understanding that potential power output is maximized when the kite angle of attack is at a ninety degree angle to the direction of the wind. Loyd estimated that a kite with an area of 2000 m^2 and 1200 m tethers has the potential of producing an average power output of 45 MW.

Dr. J. S. Goela, of the Indian University of Technology Kanpur, investigated the feasibility of a kite system to convert wind power into a usable form of mechanical energy as well as electrical energy. Goela (1983) is one of several yearly reports

chronicling the progress of Goela's research. The work in this particular publication focuses on harnessing wind power to lift a bucket of water from a deep well. After much work in the area of kite wind power, Goela proposed to design and test a system to confirm the ability of a kite system to translate wind power into usable energy. Goela (1983) stated that the dynamical analysis of kite motions and the design of the simple mechanical system proved that the conversion of wind power into either mechanical or electrical energy is a feasible option for renewable energy production. Goela's work will be further summarized in later sections.

When one considers the sport of kiteboarding, it is apparent that wind power is already being converted into a usable form of mechanical energy. Kiteboarding is a sport in which a kite is used to pull a rider on land, sea, or water. A system called a "skysail" is another kite system intended to translate wind power into a useful form of mechanical power. A skysail, shown in Figure 4, is a large kite on the order of 5000 m^2 that is believed to have the ability of decreasing the required fuel of an ocean-going tanker by as much as 20%, saving billions of dollars on diesel fuel purchases. (foxxaero, 2003)

(http://www.diseno-art.com/encyclopedia/archive/skysail.html)

Figure 4 - SkySail

1.2 Project Goals

The goal of this project was to design and construct a wind power from kites demonstrator. This demonstrator would have to consist of several key components with particular functions. The demonstrator would have to have the ability to change the angle of attack of the kite as well as convert the linear motion of the kite into a rotary motion via a power conversion mechanism.

In order for the kite to be used to convert wind power into electrical power there must be a minimum of three mechanisms incorporated into the particular system. These mechanisms are: main mechanism to change linear motion into rotary motion; angle of attack change mechanism; and kite stability control mechanism.

The main mechanism consists of several components to be discussed later operating in unison to convert the linear vertical motion of the tether into a rotary motion

of a shaft. The angle of attack changing mechanism is intended to work with the main mechanism design to change the angle of attack of the kite in order to force it to move up and down in the air, thus creating the linear force that the mechanism converts to a rotary motion. The concept of a stability control mechanism arose from the belief that a mechanism may be required to control and limit the adverse effects the wind may have on the kite due to unexpected direction changes and gusts. Though the issue of stability was addressed, the mechanism was not completely designed nor was it incorporated into the final system design. Each of the components of the system will have to work in concert in order to efficiently convert the linear motion of the kite into a rotary motion to produce energy. The design and construction of each individual subsystem will be described in detail in later sections.

In order to analyze the potential power output of the designed system several forms of simulations were performed. As previously stated, the steady state equations of kite dynamics were developed from the work of Dr. Goela. The steady state equations were used to simulate the kite in a stationary position to determine potential line tensions and power output. Dynamic simulations were also done in order to couple the steady state simulations with the specific geometries and dimensions of the designed system. To ensure that the forces applied to the designed system were not in excess a series of stress analysis calculations were performed to determine the strength of the system at several critical points. Simulations will be discussed in much more detail in future sections. In the design process software programs such as SolidWorks and Working Model were used in order to model the individual mechanisms and the system as a whole as the design progressed.

2. Background

2.1 Previous Studies

Research done in the past on the concept of using a kite for power generation was primarily done by Dr. Goela. Therefore, much of the background information providing the theory for this project has come from one of three publications by Dr. Goela; Goela (1983), Goela (1979), Goela et al. (1986). The publication that has provided much of the analytical background and the equations of motion for dynamic simulations, which will be introduced later in this report, is Goela (1983). This particular publication was one of several yearly reports compiled by Dr. Goela and his research assistants at the Indian Institute of Technology Kanpur. Dr. Goela has served as a technical consultant on this MQP project.

Goela (1983) performs analysis of the steady state motion of the kite during both stages of its motion, ascent and descent. The mathematical analysis concentrated on the forces acting on the kite and the forces produced by the kite on the system as a result of the kite motion. With the equations of kite dynamics formulated, Goela (1983) considers several other important factors in the analysis of the kite system. Goela (1983) determines the relative efficiencies of the kite system, such as the potential power coefficients, as well as the delay time between the phases of ascent and descent. .

Goela (1983) also studied the design of the kite and the mechanism to be used for the system to convert wind energy into mechanical energy. In order to develop the best kite design for their purposes, Goela and his team tested several different designs for the kites. In order to collect data, the kites were tested in a large wind tunnel and specific force measurements were taken at different angles of attack. Several different types of

kites (Figure 5) were tested in order to find the one that best suited the objective of the project and the final choice was a conyne kite (Figure 6). This type of kite gave the best overall results for the desired properties as "it incorporates the lifting advantage of a flat kite with the stability of a box kite" Goela (1983).

The second main feature of a kite-powered system is the mechanism that translates the motion of the kite into a usable form of energy. In the case of Goela (1983), the form of usable energy is the ability to raise water out of a well. The mechanism that Dr. Goela and his team designed consisted of a balanced beam on a fulcrum with spring-loaded assists as shown in Figure 7 and Figure 8. The springs in the system were used as a switching mechanism in order to chance the angle of attack of the kite, changing from ascent to descent. As the balanced beam reaches the top of its path the water is discarded from the bucket, decreasing the weight of the bucket as the angle of attack is decreased with the flip of the lever. The motion described above is portrayed in the two stage view in Figure 8. Once the angle of attack is changed the bucket is slightly heavier than the tension in the tether and the kite is pulled back down to its starting point. The cycle restarts once the lever is triggered in the opposite direction during the descent of the bucket and kite. The system of Goela (1983) was intended to lift a bucket full of water from a well and therefore cannot be directly incorporated into the work being done for this project, although as we shall see, it did influence our demonstrative analysis.

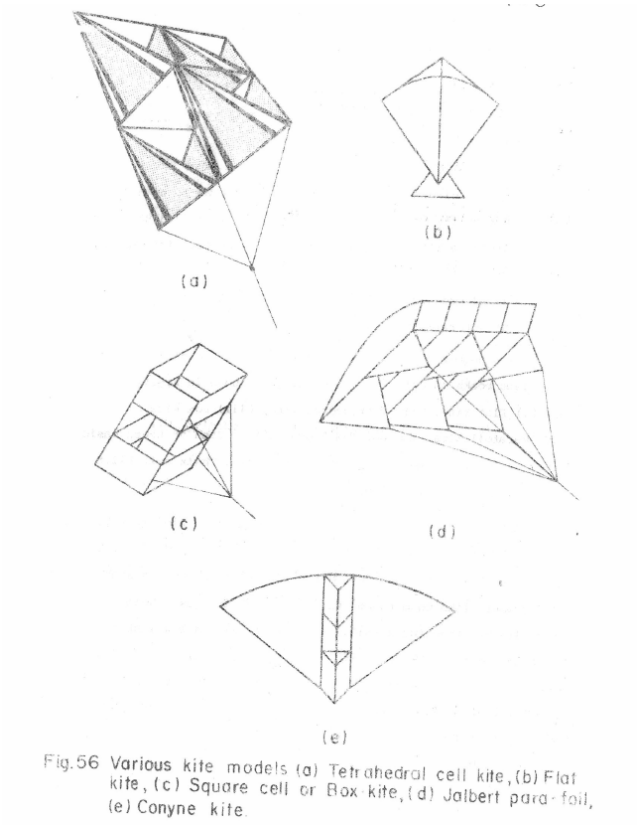

Fig.56 Various kite models (a) Tetrahedral cell kite, (b) Flat kite, (c) Square cell or Box kite, (d) Jalbert para-foil, (e) Conyne kite

Figure 5 - Early Goela Kite Models, From Goela (1983)

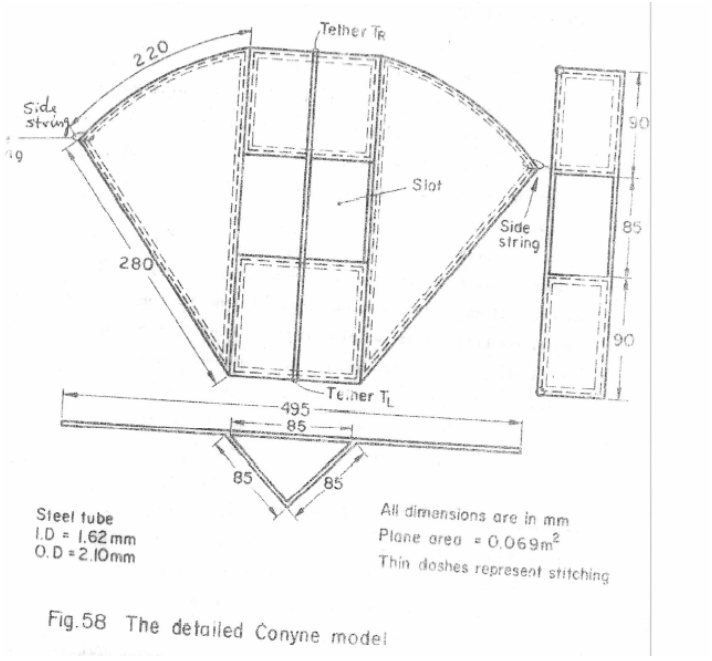

Fig.58 The detailed Conyne model

Figure 6 - Goela Kite Model, From Goela (1983)

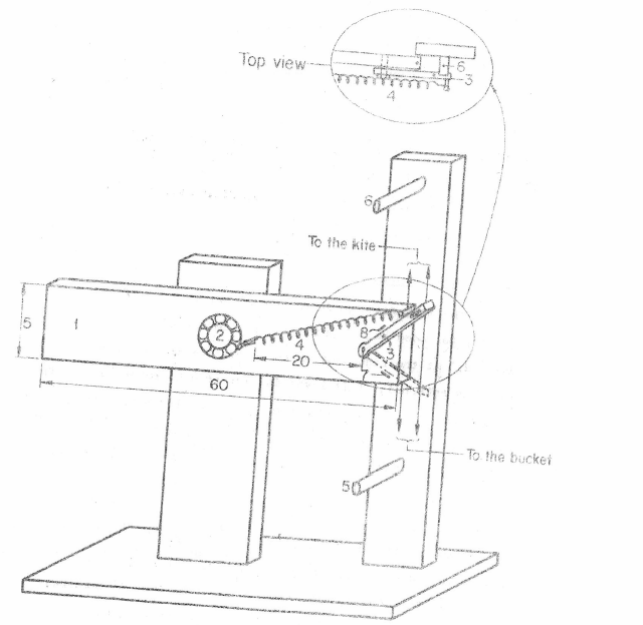

Fig.62 Details of a kite pump mechanism.
All dimensions are in cm.

Figure 7 - Goela Spring Mechanism View 1, From Goela (1983)

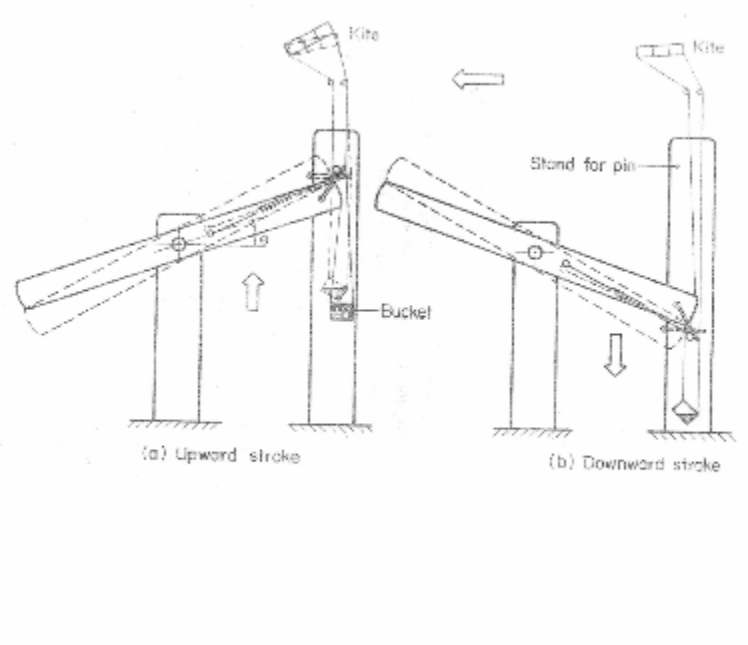

Figure 8 - Goela Spring Model View 2, From Goela (1983)

2.2 Potential Wind Power

When gauging the potential power of wind systems it is important to remember how this power is calculated. The equation for wind power is calculated using:

$$Pwind = \left(\frac{1}{2}\right) \cdot \rho \cdot A^2 \cdot Vwind^3 \quad \textbf{(1)}$$

The Vwind is the velocity of the wind, ρ is the density of the air and A is the area swept by the wind. From this equation it is evident that an increase in wind velocity results in a much higher wind power. Using the wind power equation, with potential wind power based on sea level conditions (ρ = 1.23 kg/m^3), and an area (A = 1 m^2):

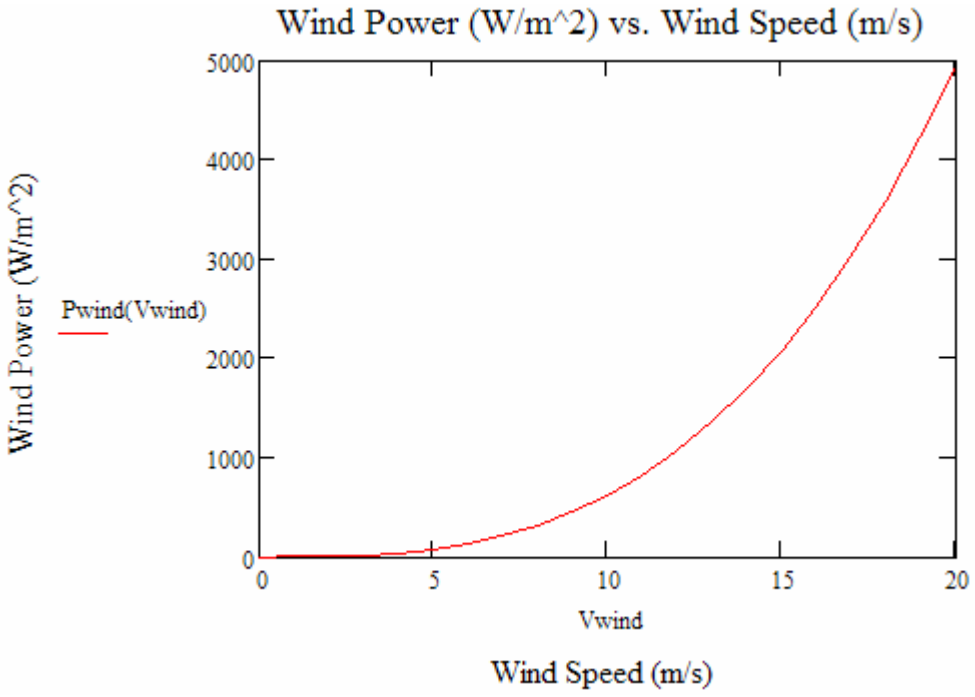

Figure 9 - Wind Power based on Wind speed

With this in mind, it becomes clear that wind power systems generate much more power in areas of high wind speed. This is why many wind turbines reach as high as 50m in height. The speed of wind tends to improve upon at higher altitudes. For specific areas, wind charts have been generated up to 100m in height. These wind charts are based upon

numerical data that has been collected and average. Here is an example of a wind chart for the New England area detailing average wind speeds at a height of 30m.

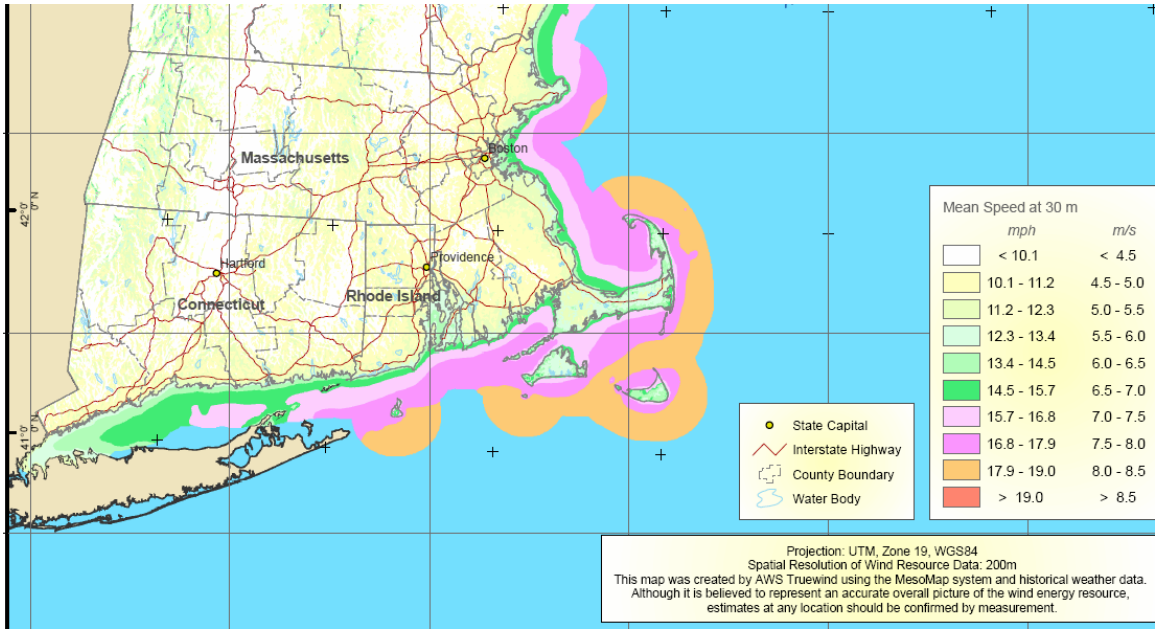

Figure 10 - New England Wind Speed 30m above Ground

Similarly, here is a chart of average wind speeds for the New England area at a height of 100m.

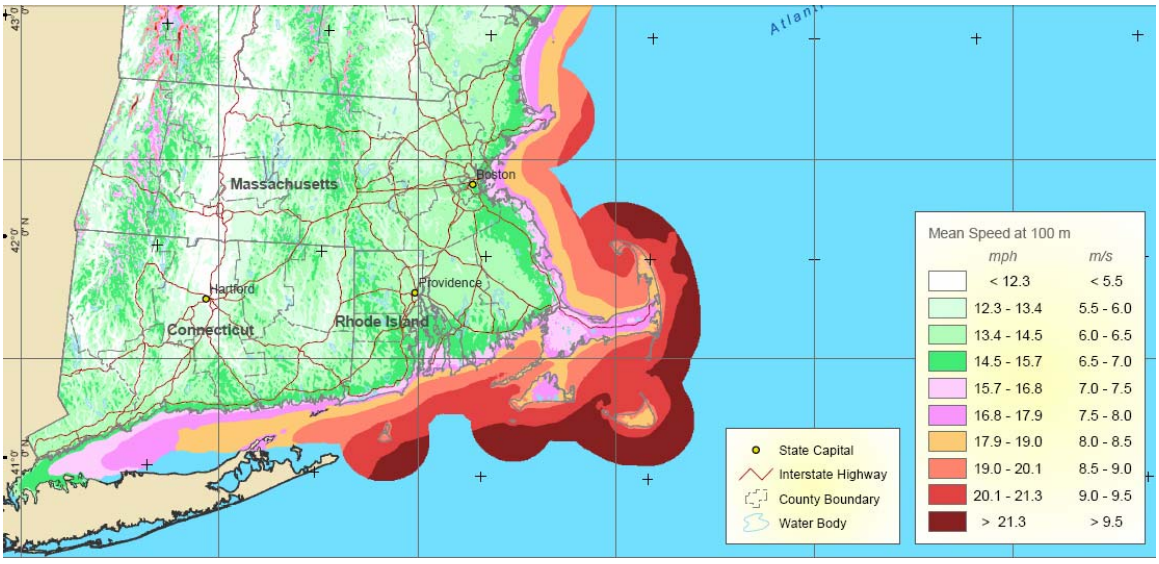

Figure 11 - New England Wind Speed 100m above Ground

Comparison of the two heights shows that the average wind speed increases by 1-1.5 m/s in a change of height of 70m. For heights greater then 100m not much data is available. For these higher heights it is generally acceptable to use the equation of the form:

$$Vwind = (Vground) \cdot (\Delta h)^{\frac{1}{7}} \quad \textbf{(2)}$$

Of course, most wind turbines cannot reach heights greater then 50m, where the potential power of the wind is much higher. There is where the use of kites can unlock the potential power found at high elevations. Kites can fly at heights up to thousands of feet depending on the area. In the United states the maximum height is regulated to 500 feet (152 meters) based on Federal Regulations. Most third world countries have little to no restrictions on the possible height of the kite. However, the potential power output at even 500 feet is still much higher than 150 feet (50m).

An example demonstrates the potential power at higher elevations. Consider two separate elevations with one at 30m, and another representing 100m. Using wind data from earlier graphs, an area of Massachusetts experiences 4.5m/s average wind speeds at 30m elevation. While the 100m elevation experiences an average wind 6.5m/s. Calculating the wind power per one square meter gives shows that 56 W/m^2 is potentially available at 30m, while 156 W/m^2 is available at a height of 100m. This change in height represents a 300% increase in the potential power. The design of our project is to harness this extra available power.

3. Methodology

The main goal of this project is to design a wind power from kites demonstrator that can be proven to generate useful amounts of electricity in a costly and efficient manner. To accomplish this goal our project was split into two design phases. First is the choice of a suitable kite that can be easily manipulated and that is readily available. The second is a mechanism that can successfully translate the linear oscillating motion of a kite into a rotary motion that can power a generator.

3.1 Kites

For our applications, the properties we are looking for in a kite are: stability, ease of use, and durability. Our original idea was to fabricate our own kite so we could design it to exactly fit our needs but due to the time involved we rejected this idea in favor of using a tested and proven kite design. We chose to use a kite that was designed specifically for kite boarding, a sport where the rider is towed across the ground or water by a kite, relying only on a light wind for acceleration. These kites come in a variety of sizes, ranging from 2 square meter trainer kites to 20 square meters for heavier riders, with most riders using between a kite between 9 and 13 square meters. The kites operate in what is called the power zone, or the area in which the kite gets the most lift. The power zone is typically defined as a half-hemisphere stretching 180 degrees in front of the rider and projecting 90 degrees down in an arc from the vertical direction. The advantage of a large kite is that it will provide line tension at higher wind speeds and is more stable when aloft due to its greater area. The smaller kites have an equal advantage

at lower speed winds, requiring only a light breeze to keep them aloft, but are less stable due to their smaller profile.

Kite boarding kites employ several different control systems, ranging from the simple 1 line system of a traditional kite to a 5-line system of some of the more advanced kite-boarding kites. Typically, most kite boarding kites have either a 2 or 4 line configuration. In a 2-line setup, two lines are attached to the kite, usually to a bridal system that then spreads out to the underside of the kite. The downside to this system is that only the roll motion of the kite can be altered, not the angle of attack. Because of this, we immediately rejected any kite with this type of system, since our project relies on changing the kite's angle of attack. The other line configuration, a 4-line system, has a line at each corner of the kite.

The most commonly used type of kite boarding kite is the traditional parafoil. This type of kite consists merely of two sheets of rip-stop nylon with vertical strips of nylon uniting the two. The air is allowed to move between the top and bottom layer of the parafoil and gives it its structure. This kite is normally found in a 2-line variety, but can come in 4-line. In kite boarding, this type of kite is traditionally used as a trainer kite to train riders how to control the kite. The downside of this kite was that it was unstable, requiring constant supervision and roll adjustments to keep it within the power zone.

A Lead Edge Inflatable, or LEI kite, was also researched. The LEI features a leading edge and supporting struts that can be inflated and pressurized to provide rigidity and create an airfoil-like shape to the kite. However, LEI kites have only rip-stop nylon sheets in between the inflated struts, which cause increased drag due to the ability of the kite to flex, changing the geometry of that trailing edge and causing it to flutter up and

down. The advantage of this particular kite for kite boarding is that if the kite hits the water, it will stay above the surface due to the ballast from the inflatable edges. We considered this type of kite with the intention of filling the leading edge and struts with helium in order to keep the kite aloft in the event that a constant wind was lost. We later rejected this idea due to the amount of helium needed to keep the kite aloft, and exotic materials that would have to have been implemented to ensure the helium did not leak out. Overall, these kites were generally stable, but did require constant trim to keep them in what is called the power zone.

Another kite commonly used by kite boarders was a Bow kite, which is a slightly modified version of the LEI. With a bow kite, the leading edge lines run across the interior body of the kite, giving the rider the ability to control the front profile of the kite, thus reducing or increasing the effective surface area that the wind can act upon and thereby increasing the kites operating wind ranges. These kites however are notoriously unstable and sensitive, and as a result, we eliminated them as a choice due to the amount of attention they needed to be operated.

Kites manufactured by Peter Lynn, Inc. were also considered. The design of this kite utilizes an unpressurized inflatable structure, whose profile mimics that of an airfoil. The advantage of this design over a lead edge inflatable kite is that the since the kite mimics an airfoil, it has an uninterrupted air flow pattern over both sides of the kite, as opposed to a LEI kite, which has a continuous line over the top edge, but a stagnation point on the bottom edge shortly after the air passes the front bladder, as seen in Figure 12.

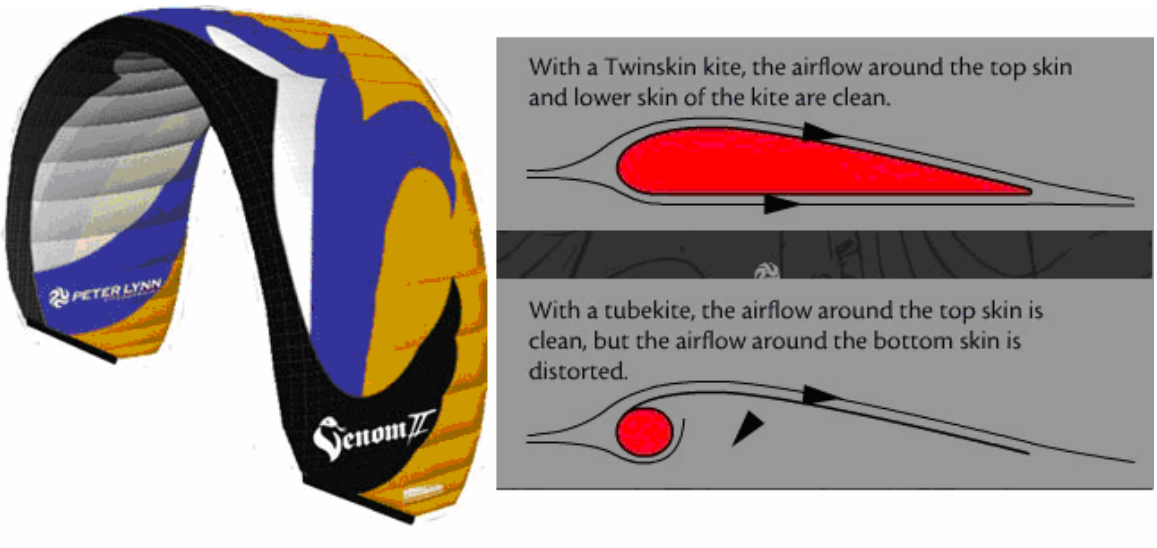

Figure 12 - Peter Lynn Venom and Twinskin Technology explained

Additionally the Venom also has a feature called an auto zenith, which enables the kite to re-launch itself in the event that it falls out of the power zone. This feature also ensures that when the kite is at rest and without any rider intervention, the kite stays at the zenith with minimal perturbations.

3.1.1 Kite Purchase

As mentioned in the previous section, a four-line kite provides enough dynamics to keep the kite stable and under control. Four lines are also necessary to ensure that the kite's angle of attack can be successfully controlled. More than four lines would be unnecessary because the addition of more lines provides little to gain in the kite's control. With four lines and an auto-zenith stability feature, it was found that a Peter Lynn Twin-skin kite would be best for the purposes of the project.

Peter Lynn Kites are very difficult to find at retailers and very expensive for the new factory versions. To reduce costs it was decided to find a relatively cheap, rarely used Peter Lynn kite from either the kite boarding community or a host of various Internet locations. Eventually, a Peter Lynn Guerilla 10 m^2 kite was found and purchased on EBay for $300.00. According to the seller the kite was flown only once, and personal inspections of the kite showed that it had very little use. This kite was purchased for a relatively low price as a new Peter Lynn Guerilla costs approximately $800.00. Figure 6 shows the 12m^2 version of the Peter Lynn Guerilla.

Figure 13 - Peter Lynn Guerilla

Some of the Kite Specifications:

Kite Area (m^2)	10 m^2
Kite Weight (N)	22.24
Chord Length (m)	1.575
Wingspan (m)	7.62
Aspect Ratio	4.84
# of Control Lines	Four
Minimum Required Wind Speed (m/s)	3 m/s
Maximum Wind Speed (m/s)	13 m/s

Table 1 - Peter Lynn Guerilla 10m^2 characteristics

3.1.2 Kite Testing

To become more familiar with the use and control of the kites, several trips were taken to a local kite shop, Powerline Sports in Seabrook, NH owned by Andrew Ghezzi, where the proper use and control of large sport kites were demonstrated. These trips were also used to find the kite line tension capabilities and the resulting coefficients of lift that sport kites can generate. For smaller kites with less lifting capability a simple setup was created:

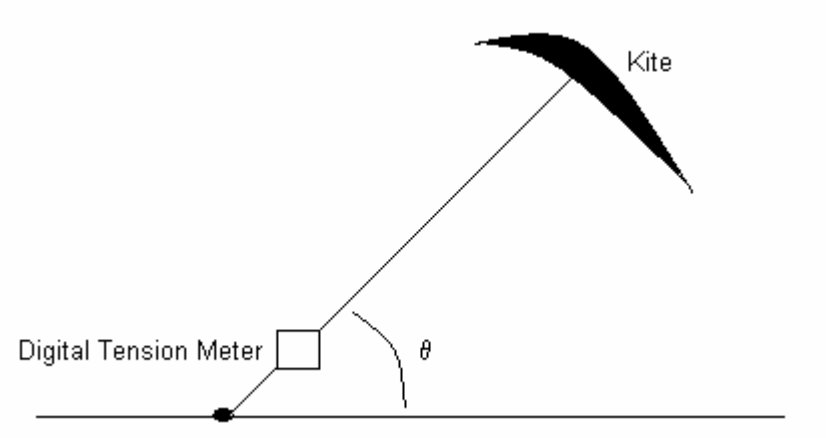

Figure 14 - Beach Kite Testing

In this setup, the kite is attached to a digital tension meter that is then attached to the ground. The readout of the digital tension meter allows us to find the line tension. Since the four line kites have the ability to control angle of attack, several tension measurements were taken for various angles of attack. A digital angle meter was used to measure the angle θ in the diagram, which was used in turn to determine the kite's approximate angle of attack. However, one problem with our experimentation is that it is nearly impossible to measure a kite's angle of attack while it is in flight. To fix this

problem it was assumed that the angle of attack during the kites De-Powered Mode (0 line tension) is zero and that the angle of attack during Powered Mode (maximum Line Tension) is 90 minus the angle theta that is measured at the ground.

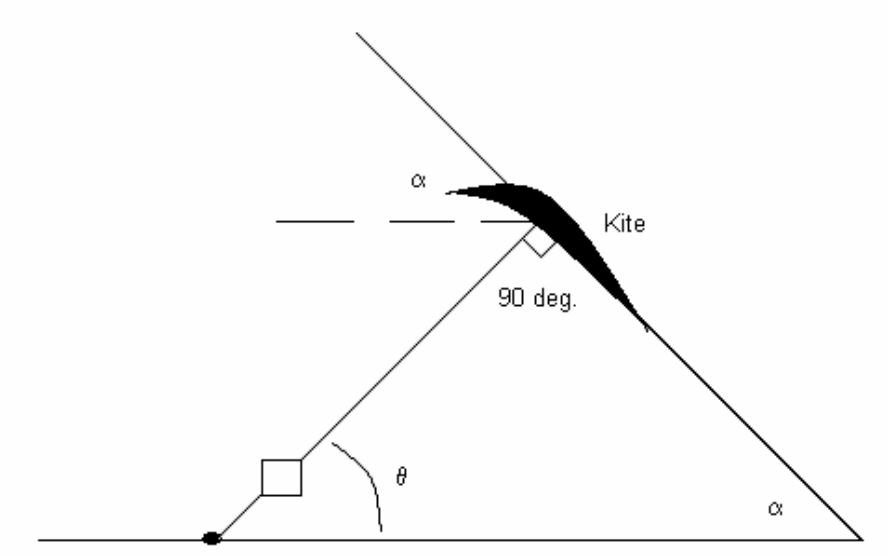

Figure 15 - Angle of Attack Approximation

From the above diagram the angle of attack is approximated by:

$$\alpha = 180 - 90 - \theta \qquad \textbf{(3)}$$

This approximation is not always accurate because the parafoil could already be at an angle when it is in the De-Powered mode. However, for our purposes the approximation was accurate enough to determine a general form of several kites lift vs. Angle of Attack ratios.

The one difficulty with this setup is that the digital tension meter was only capable of measuring forces up to 60 pounds, when these kites were capable of lift well over one hundred pounds. Therefore, for larger kites the digital tension meter was replaced with a large industrial spring. By calibrating the spring to find its appropriate spring constant, the kites lift was found by measuring the spring's deflection.

3.2 System Design

A design process was conducted consisting of three steps to design the power from kites demonstrator. First, we created a list of possible system designs. Next, each design was evaluated until a final design mechanism was chosen based on several criteria. Finally, the system was visualized using SolidWorks software.

3.2.1 Possible Mechanism Designs

To harness the available energy in an oscillating kite system, it is necessary to design several mechanisms. The mechanisms that are required can be divided into three separate categories; Angle of Attack Control, Energy Conversion, and Roll Control. Though, the roll control mechanism was not completely designed in this project efforts were made to address its potential design and function.

Angle of Attack Control

All of the potential energy conversion mechanisms require that the kite is oscillating in a consistent up and down motion. To create this kite motion a mechanism is required that will change the kites angle of attack. Modern kites used in the sport of kite surfing have a standard setup that is used to control a kite's angle of attack. Since these modern angle of attack mechanisms are proven to operate successfully, it was decided that it would be ideal to incorporate this existing technology into the attack change mechanism.

The standard angle of attack control for a four-line sport kite is shown below:

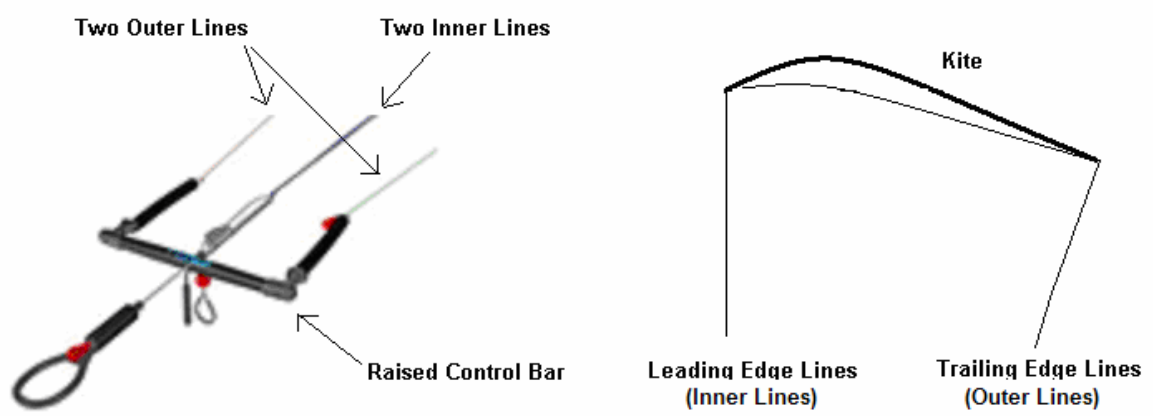

Figure 16 - Modern Kite Control System in a De-Powered State

In the picture above, the inner line splits into two lines that are connected to the leading edge of the kite while the outside two lines are connected to the kite's trailing edge. The inner two lines run through an opening in the control bar, allowing the bar to slide along the two inner lines. In this type of control system the two inner lines provide the major pull of the kite and the outer two lines connected to the control bar provide angle of attack control. When the control bar is raised outward (Figure 16), the kite is in the "De-powered" state, meaning that the Kite's angle of attack is near zero and that the kite is offering little or no pull. In this De-powered state the kite is effectively level and all four lines connecting to the kite are at the same length. When the control bar is pulled close to the rider as seen in Figure 17, the kite is in the "Powered" mode and the kite is at full pulling force. In this instance, the trailing edge of the kite has been pulled downward increasing the kite's angle of attack. The two outer lines on the control bar can also be 'trimmed', in other words the line lengths can be shortened to a desired length by simply

tying knots in the cord that the lines attach to. The purpose of altering the length of the lines is to optimize the kite's L/D (lift/drag) and thus improve its overall performance.

When controlling the angle of attack of the kite, two significant conditions must be considered. The upper and lower bounds of the control of the angle of attack are two issues known as 'undersheeting' and 'oversheeting'. Undersheeting is the condition at which the kite is at an angle of attack providing an insufficient amount of lift. In this state the drag is greater than the lift on the kite and therefore the kite is unable to lift and produce significant power. Oversheeting is the condition in which the angle of attack has increased beyond the angle of attack that coincides with the highest value of L/D. At this point the kite begins to become less powered, and eventually depowered, as the angle of attack increases beyond the maximum corresponding L/D.

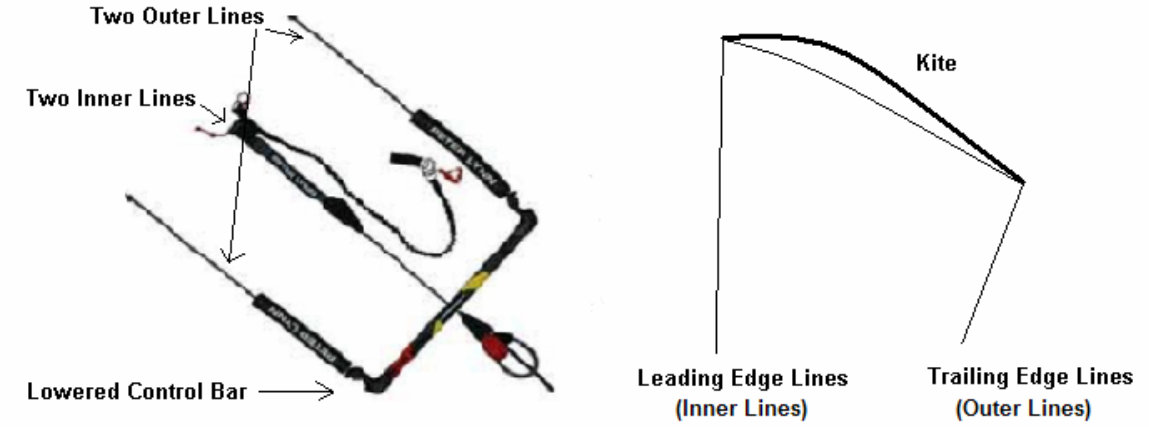

Figure 17 - Control Mechanism in a "Powered" State

Energy conversion

The conversion of mechanical energy to electrical energy will require the use of a mechanically driven electrical generator. However, there needs to be a mechanism that can convert the oscillating motion of a kite into rotary motion that can power a generator. Several possibilities for such a mechanism were considered.

The simplest conversion mechanism is a simple lever. A simple lever would be a beam attached to a kite that would spin around a shaft powering an electrical generator.

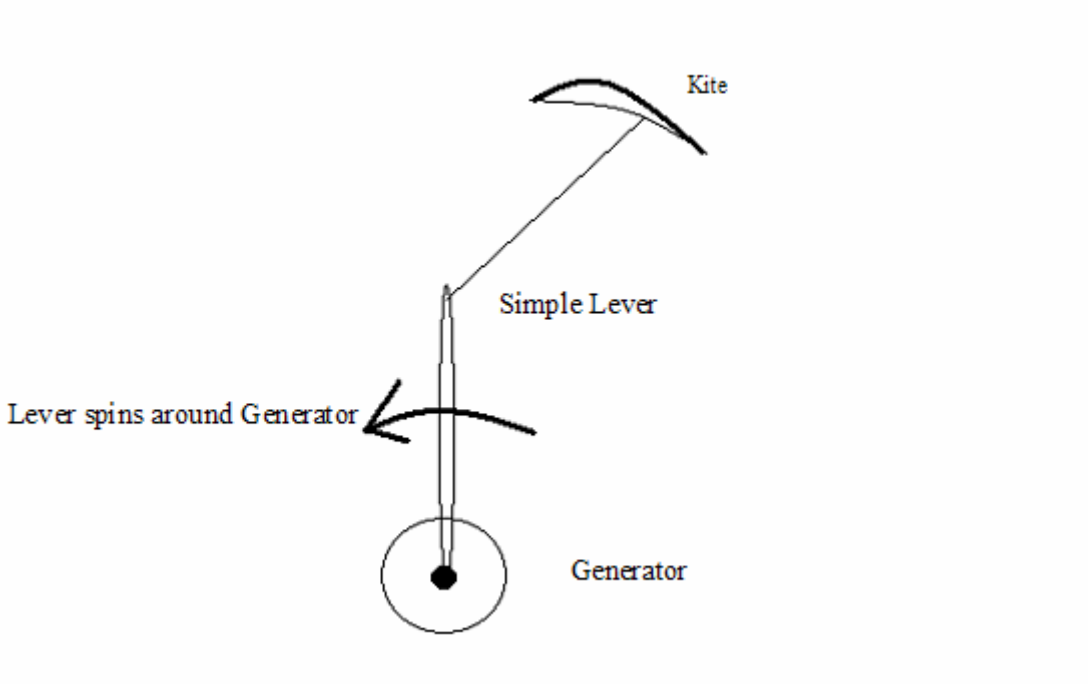

Figure 18 - Simple Lever

The major advantage of this system is simplicity of construction. However, this system was found to have several disadvantages. One major disadvantage is the system's inability to have the simple lever rotate in a complete circle. The shaft would require enough momentum to keep revolving, while the kite would need to be put into "de-

powered" and "Powered" positions at key points in the revolution of the lever. This turns out to be an extremely difficult task.

Another similar mechanism is a reversing simple lever. In this mechanism, the kite would move the lever from side to side. The end of the lever attached to the generator shaft would also be connected to a reversing clutch. This clutch would make sure that the motion of the generator shaft only moves in one direction. An advantage of this system is that the lever does not need to completely revolve around the entire assembly. The angle of attack would change moving the lever from one side to the next. However, a concern with this system is that it cannot sweep enough of an arc to have the lever cause any significant torque upon a gear system.

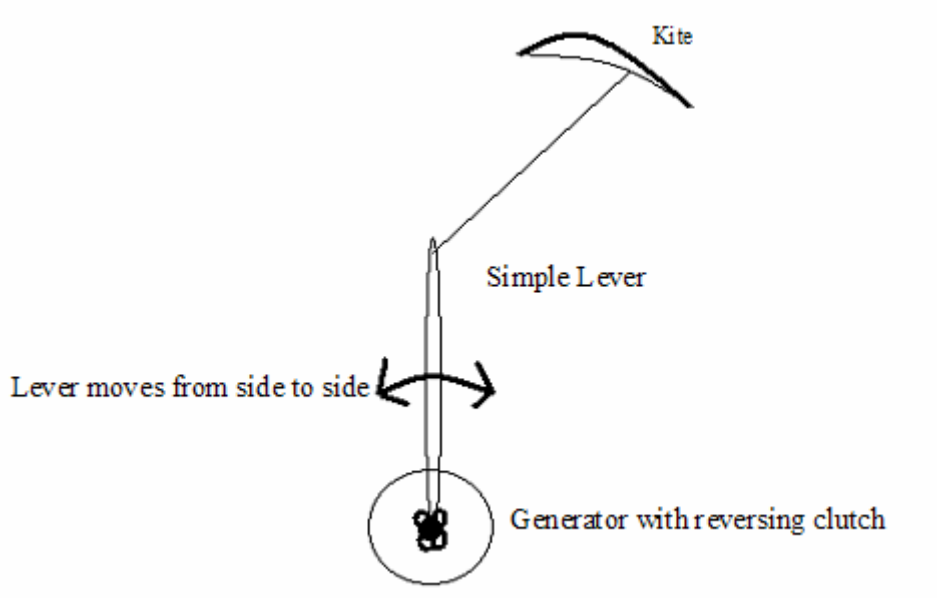

Figure 19 - Simple Lever Reverse Clutch

Another possible mechanism consisted of a two-kite system. The two-kite system involves two kites that work together to move the shaft of the generator. This can be accomplished in several ways. Two kites could run the reversing simple lever mechanism

shown in Figure 19. Two kites could also be made to move in a circular motion that could power a generator as in Figure 20. The difficulty of the two-kite system is the added complexity. The kites could move around each other and twist together. It also becomes more complex to control the motion of the kite. If the two kites aren't configured properly their motions could counterbalance each other.

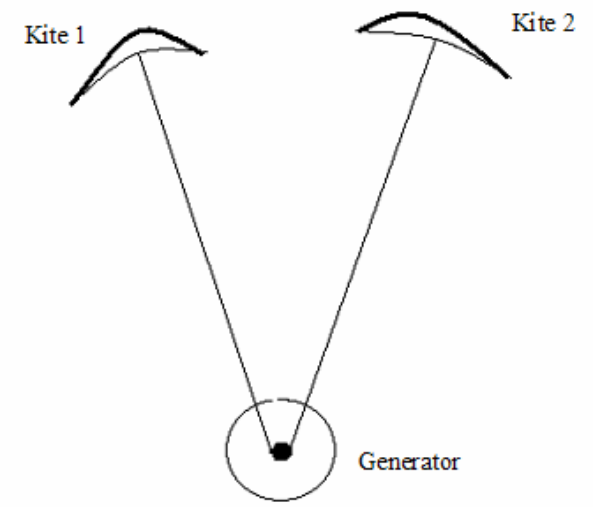

Figure 20 - Possible Two-Kite System #1

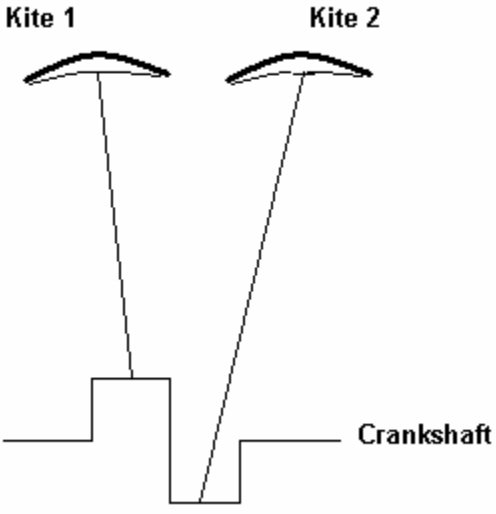

Figure 21 - Possible Two kite System #2

There are also several classical mechanisms that have been used to convert oscillating motion into rotary motion and vice versa. One of these mechanisms is the pump jack. The pump jack is the mechanism used to pump oil from oil wells. An example of a pump jack is shown in Figure 22.

Figure 22 - Oil Pump Jack

In the case of the pump jack, a motor creates a rotary motion the moves the left side of the beam up and down, causing the right side of the upper beam to move up and down in an oscillating motion. In the case of our project, the up and down motion of the kite would move the right side of the pivoting beam up and down which would then drive the beam that causes the rotary motion. This rotary motion would then drive the generator.

Other possible mechanisms involve the use of spring systems. This spring systems would rely on the use of a sprag clutch. A sprag clutch is the mechanism that

allows a ratchet to apply a force in one rotational direction and not in the opposite direction. An example of a possible system using a sprag clutch can be seen in Figure 23:

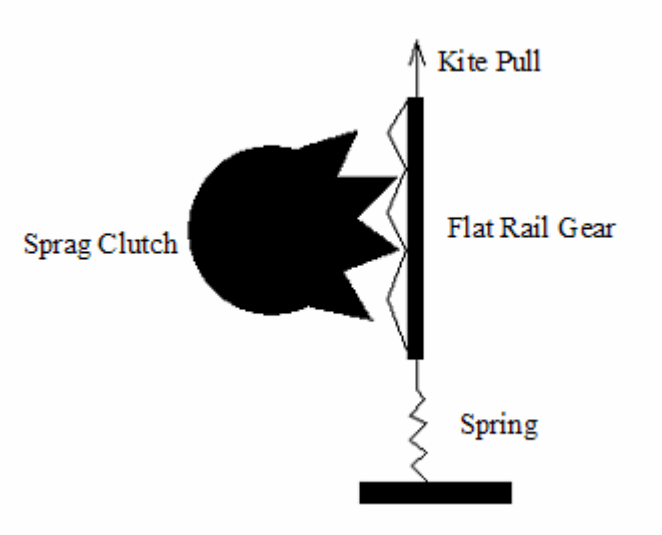

Figure 23 - Example Sprag Clutch

In a sprag clutch system, the kite would pull the flat rail gear that is positioned to move up and down. When the kite is put into the power mode, the kite would lift the rail upward, turning the large round gear and eventually spinning an electrical generator. When the rail gear reaches a maximum height, the kite is triggered to change into "de-power" mode. Once this happens the kite loses its upward pull and the spring pulls the kite along with the rail gear back down into the starting position. As the gear rail moves downward the gear moves back down but does not affect the gear shaft motion. When the kite reaches the starting position, the kite is triggered into power mode and the cycle starts all over again.

The last possibility considered was the combination between the sprag clutch and the large rotating beam found on the pumpjack. The idea is that a kite would be attached

to an oscillating balanced beam. When the kite was in the down position it would increase the kites angle of attack and the beam would be lifted upward by the kites motion. When then beam reached the top of its arc, a sliding weight inside the rotating beam would pull the angle of attack control strings downward, decreasing the kites angle of attack. The weight within the beam would then pull the beam back down to starting position. The Sprag clutch will come in to play when the beam is in its upward trajectory. While the beam is moving upward it will be pulling a chain which is spinning a sprag clutch that in turn leads to a gearbox and eventually a generator. A schematic of this is shown here:

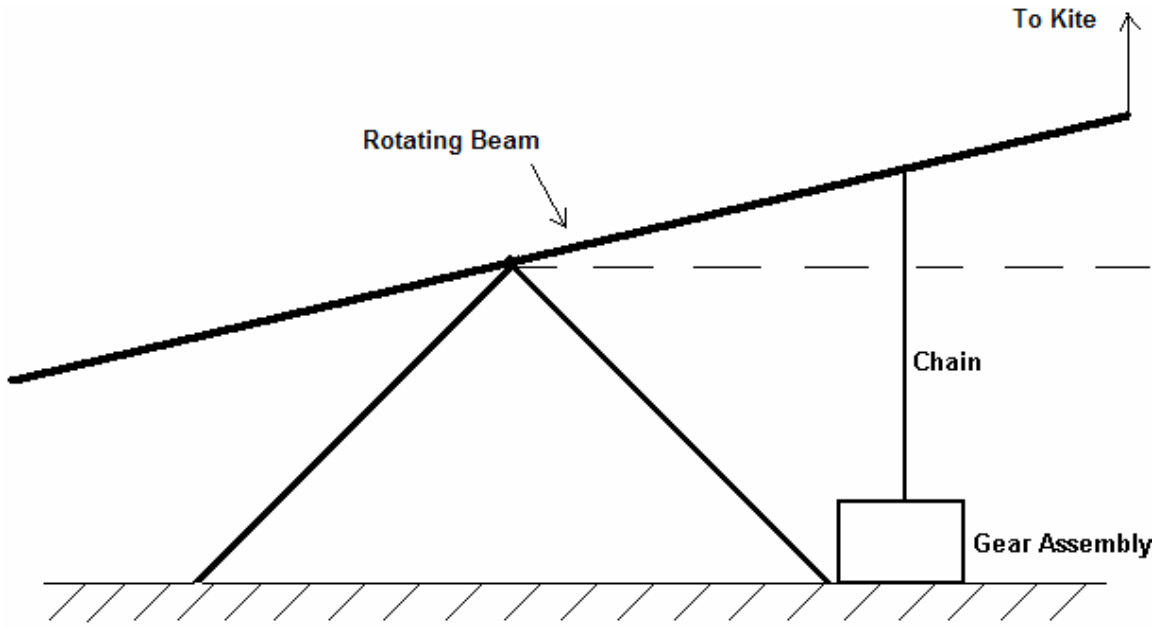

Figure 24 - Pumpjack/Sprag Clutch Combo

Roll Control

One possible problem with the kite motion is the kite's ability to roll, or move side to side. This problem must be dealt with in order to maintain the oscillating motion of the kite and to prevent line tangling or even the total collapse of the kite in the air. In

order to control the roll of the kite, a simple mechanism can be integrated into the construction of the overall system. An example of a simple mechanism that may control the roll of the kite may be the addition of a spring system that will adjust for different tensions in the lines of the kite. This type of system is shown here:

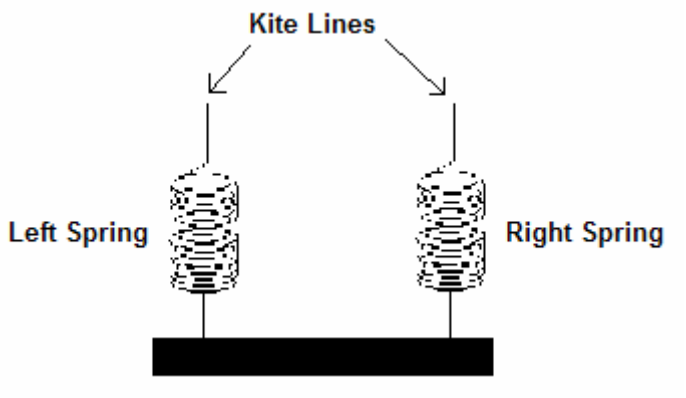

Figure 25 - Possible Roll Control Spring Mechanism

If the kite is farther to one side than the other the tension in the far side line will be greater, and will in turn increase the spring force. A higher spring force will pull the kite back to that side with a greater pull than the side with a lower force, ultimately evening out the position of the kite in the air and preventing an excessive amount of roll. As previously stated, the issue of roll control has been addressed but it has not been fully developed nor has it been incorporated into the demonstrator design thus far.

3.2.2 Mechanisms Evaluation

After careful consideration of the possible design mechanisms, it was decided that the two simple lever designs were the least likely to generate high amounts of power, because they create low amounts of torque and rpm required to power a generator. These two concepts were removed from the possibilities as well as any of the two-kite designs.

Two-kite designs are certainly feasible, but they are much too complex and costly for this project.

With the elimination of a few of the possible design alternatives, the final choice for the energy conversion mechanism system was limited to three different design concepts. These three mechanisms were the Pumpjack, the Sprag Clutch and The Pumpjack/Sprag Clutch Combo. To decide which mechanism provides the most benefit, a comparable evaluation of all three mechanisms was conducted. The evaluation process is described in the following section.

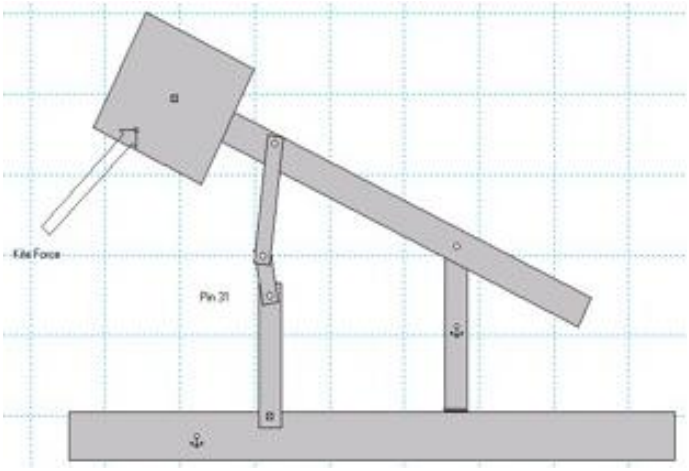

Figure 26 - Illustration of Pump Jack Design

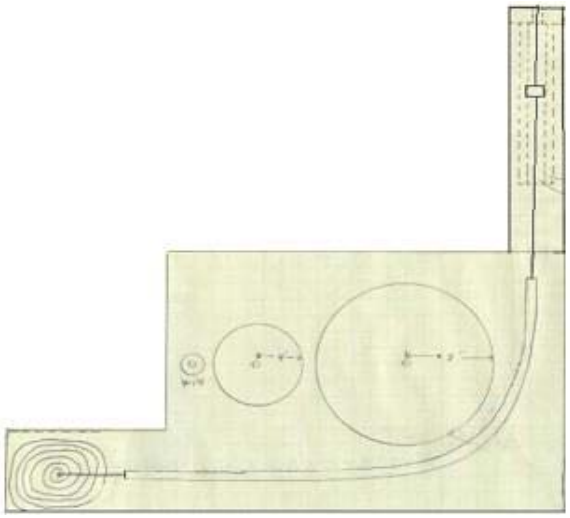

Figure 27 - Illustration of Sprag Clutch Design

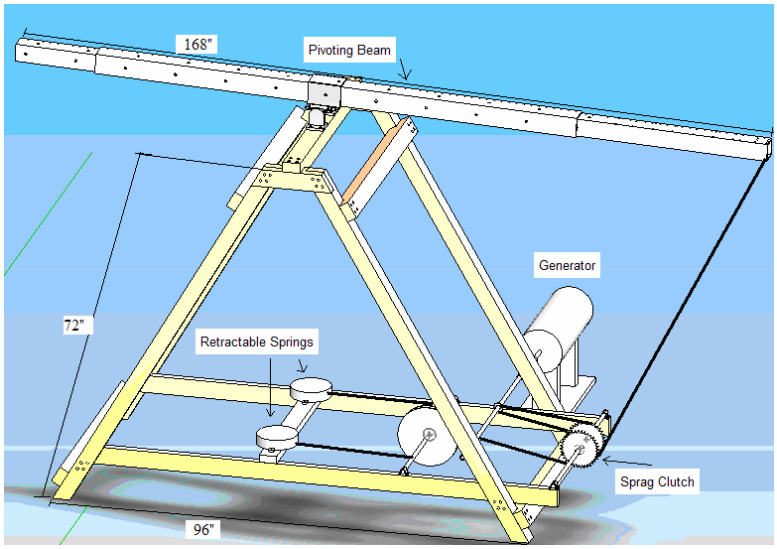

Figure 28 - Illustration of Sprag Clutch / Pump Jack Combo Design

Evaluation Scale

The scale in Table 2 was used to rate each system for a given criteria. The values were assigned to each category with scores being awarded to each mechanism in comparison to the other two mechanisms. In cases where the difference between two mechanisms is indistinguishable, both mechanisms were awarded the same value.

Subjective	Value	Description
Good	**3**	**Exhibits traits better than other mechanisms**
Medium	**2**	**Traits fall between two other systems**
Bad	**1**	**Exhibits traits worse than other two systems**

Table 2 - Evaluation Scale

Evaluation Criteria:

1. Potential KW – The system with the potential to generate the most electricity. This mechanism has the ability to harness the most mechanical power over a given time period. The mechanisms ability to produce power at lower wind speeds was also considered.

2. Scalability – The potential for these systems to be scaled into larger systems. This includes issues such as springs that lose their potential with size, and the functioning of inner components of the system.

3. Practicality – The systems ability to be constructed and maintained. This includes the availability and production methods included in the construction of the system.

4. Autonomy – this criterion assesses the systems ability to run without the aide of any outside support. Criterion includes possible issues arising from in-climate weather and varying wind speed.

5. Manufacturing – System ability to be constructed at low cost in a reasonable amount of time. This includes complex parts that are already available or need to be specifically machined.

6. Prototype cost – The predicted cost of each system based on the systems materials and predicted times of construction.

7. Complexity – The systems complexity of design, including complexity of parts and complexity of construction.

8. Variable Wind Speed – The mechanisms ability to operate over a large range of wind speeds.

9. Demo Ease – ease of demonstration - A guess on which prototype would have the highest chance of succeeding based on several evaluation categories already mentioned.

10. Going to Operation – The probability that this mechanism could be used in the rural areas where farmers or local inhabitants could build this system for power generation. This includes availability of construction materials and costs relative to other alternative energy solutions.

11. Variability in Wind Direction – How well the mechanism will operate when the wind direction changes from direction to another. This includes how the mechanism will react when it is run with no supervision.

12. Stability Control – This assess the mechanism ability to recover after a large gust of wind moves the kite in a direction that hinders the operation of the mechanism. Also includes how easily a spring stabilizing system could be added to the mechanism.

Scoring Chart

	Pump Jack	**Sprag Clutch/Tower**	**Pump Jack / Sprag Clutch Combo**
Potential KW	Potentially higher output with desired constant shaft rotation **Score: (3)**	Relatively lower output due to non-powered down stroke **Score: (1)**	lower output due to non-powered down stroke, longer stroke **Score: (2)**
Scalability	As size of beam is increased potential power is increased **Score: (3)**	Too many variables to consider in scaling system **Score: (1)**	Similar to Pump Jack, as size is increased stroke increases **Score: (2)**
Practicality	Issues with required harmonic motion **Score: (1)**	Complexity of AOA change mechanism **Score: (2)**	Removes technical issues from each system

			Score: (3)
Autonomy	After temp. stall, unknown direction or status of operation of rotating shaft **Score: (1)**	After temp. stall, retraction mechanism should reset the kite cycle **Score: (2)**	After temp. stall, retraction mechanism should reset the kite cycle **Score: (3)**
Manufacturing	Simple, but larger components **Score: (2)**	Simple and relatively inexpensive components **Score: (3)**	Simple components, both large and small **Score: (1)**
Prototype Cost	Net cost of structure, e.g. aluminum tubing **Score: (3)**	Relatively cheap with surplus parts, sprag clutch, control bar **Score: (1)**	Aluminum tubing, sprag clutch, gear, chain **Score: (2)**
Complexity	Simple design with a complex motion **Score: (2)**	Complex AOA mechanism design, simpler motion **Score: (1)**	Combo of the best properties of each mechanism **Score: (3)**
Variable Wind Speed	More variables that have to change with wind speed (masses) **Score: (1)**	With spiral spring, variable wind speed is handled **Score: (3)**	Has spiral spring yet the large arm has masses to deal with **Score: (2)**
Demo Ease	Too many variables to consider **Score: (1)**	Complexity of AOA mech. may inhibit proper operation **Score: (2)**	Complexity of tower and rotation eliminated, more reliable operation **Score: (3)**
Going to Operation	Components of system may be readily available **Score: (2)**	AOA mech. is a complex system making application more complicated **Score: (1)**	Least complicated, least # of issues, could be used in simple applications **Score: (3)**
Variability in Wind Direction	Different tether angles may effect the operation of the AOA change mechanism **Score: (2)**	Kite tether comes out of tower mechanism, keeping the movement in the same direction no matter the angle of the line. **Score: (3)**	Different tether angles may effect the operation of the AOA change mechanism **Score: (2)**

Stability Control	May be complex to incorporate spring system onto pump jack arm **Score: (2)**	Spring concept may work best with tower system **Score: (3)**	May be complex to incorporate spring system onto pump jack arm **Score: (2)**
TOTAL:	**23**	**23**	**28**

Table 3 - Evaluation Matrix

Qualitative Scale: Best mechanism (3), Second Best Mechanism (2), Third Mechanism (1)

Total Scores:
PumpJack: **23**
Sprag Clutch: **23**
Pumpjack/Sprag Clutch Combo: **28**

Detailed Evaluation of Criteria

This section gives a detailed explanation on why values were assigned to a system for each evaluation criterion.

Potential KW

The pumpjack scored the highest rating in this category because the pumpjack provides energy to the generator in both the ascent and descent mode of the kite. The other two mechanisms both received half of the pumpjack score because they only have the potential to convert energy during the ascent stage, which is significantly less than the pumpjack capabilities.

Scalability

The Pumpjack has the best scalability because it could potentially increase in size as long as the kite providing the power was increased as well. However, both the Sprag Pump and the combo are limited by the retraction mechanism that fails to operate correctly when the system reaches a given size or dimension.

Practicality

The Pumpjack scored the lowest because it requires the most detail in design. CAD simulations of this system show that it has problems running smoothly unless the force of the kite is within a specific range. The Sprag clutch was second because of its complex angle of attack mechanism. The Combo scored the highest because it removes the technical issues from each of the other two mechanisms.

Autonomy

According to our modeling of the pumpjack system, it has the most difficulty in running efficiently. The Pumpjack requires precise sizes and weights to effectively run autonomously. This means that this system would require adjustments anytime the wind shifted in speed.

Manufacturing

The Sprag clutch scored the best due to its ability to be manufactured in a compact form with most of the component easily available. The Pumpjack was rated second because of the larger components that would need to be machined in order to function properly. The Combo scored last due to difficulties already mention in both the Pumpjack and the Sprag Clutch.

Prototype Cost

The shear size of the Pumpjack makes it the most expensive unit. The pivoting arm on the pumpjack system would need to be made of aluminum tubing to be lightweight and withstand the various stresses applied during operation. The least expensive system would be the sprag clutch. It requires the most complex building

procedure but it is the smallest system and requires the least amount of materials. The combo scores in the middle because it comes both the inexpensive and expensive parts

Complexity

The Sprag Clutch is the most complex system because its angle of attack mechanism has intricate mechanisms. The Pumpjack is the second most complicated because the pumpjack needs to be fully adjustable to correctly operate in a full range of wind speeds. The Combo scores the highest because it replaces the complex machinery present in both the Pumpjack and the sprag clutch to easily operate in most conditions.

Variable Wind Speed

The sprag clutch rates the highest in this category because of its swiveling arm capability. The swiveling arm allows the system to operate even when the wind is changing direction. The Combo ranks second because the changes in wind direction may affect the performance of the beam moving up and down. The Pumpjack scores last because during simulations adjustments of wind direction on the run caused the pumpjack to work inefficiently.

Demo Ease

The pumpjack is the hardest system for demonstration because of the number of variables required for operation. The second hardest is the Sprag Clutch because of the complex angle of attack mechanism. The simplest system is the Combo that is comprised of the easiest parts of the two more complex mechanisms.

Going to Operation

The Combo is the least complex with the least number of issues. The Pumpjack materials are the easiest to find, but it requires complex adjustability to become practical.

The sprag clutch is the least operational because it requires the more complex tower be built, which is difficult for a rural area to produce.

Stability Control

The most stable would be the Sprag clutch because of its ability to point towards the wind direction. The other two systems might not be affected in the same manner because if the kite is pointing the wrong way the springs might not be able to properly keep the kite stable.

Conclusion

Our conclusions show that the Sprag combo would be the most practical system to build. Not enough decisive evidence was found to prove that the pumpjack system would successfully operate at an effective capacity. The Sprag clutch would be the most elegant design, but the Sprag combo would accomplish the same amount of energy transfer with a simpler Angle of attack mechanism. In the next section we will discuss detailed blueprints of our Sprag combo design.

3.2.3 System Design

Once the sprag combo design was chosen, a CAD schematic of the design was created using SolidWorks software. The purpose of the SolidWorks schematic was not to create a detailed blueprint of the system, but rather a framework for the system's construction. A screenshot of the SolidWorks design is shown in Figure 29.

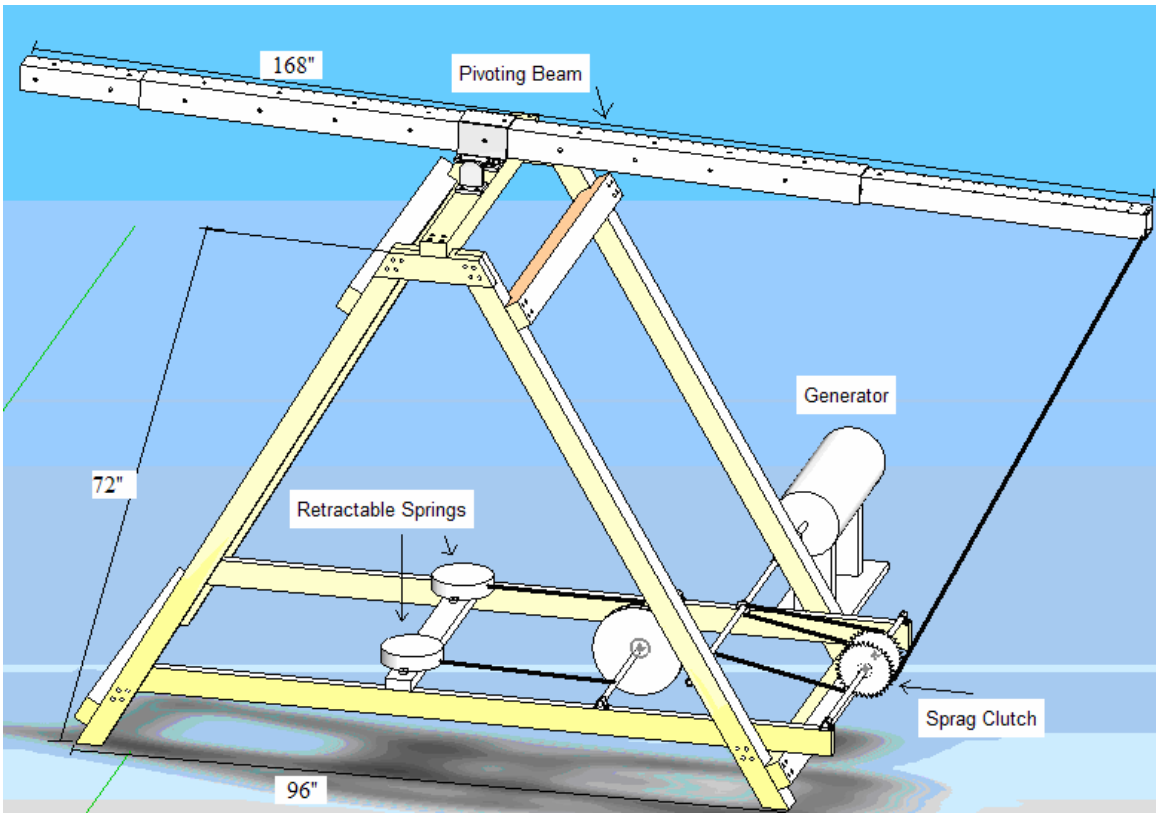

Figure 29 - AutoCAD system Model

Figure 29 shows the initial design for the sprag combo system. The wooden structure provides support to the rest of the system. The base structure was designed with a wide base to prevent possible flipping from front to back during operation. A system stress analysis provided in the results section shows that the structure can withstand the potentially high stresses applied during operation.

The aluminum pivoting beam on the top of the structure is actually composed of three separate beams. There is a large central beam with telescoping beams placed at each end. An exploded view shows the beam in more detail.

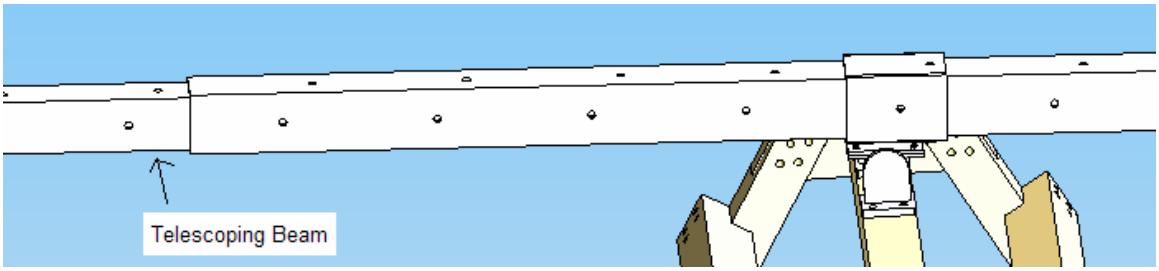

Figure 30 - Telescoping Beam

The telescoping beams and the large central beam all have aligned holes drilled through them. Bolts can be placed through the various holes to change the overall length of the beam.

One essential portion of our design was the angle of attack mechanism. Our original concept can be seen in Figure 31.

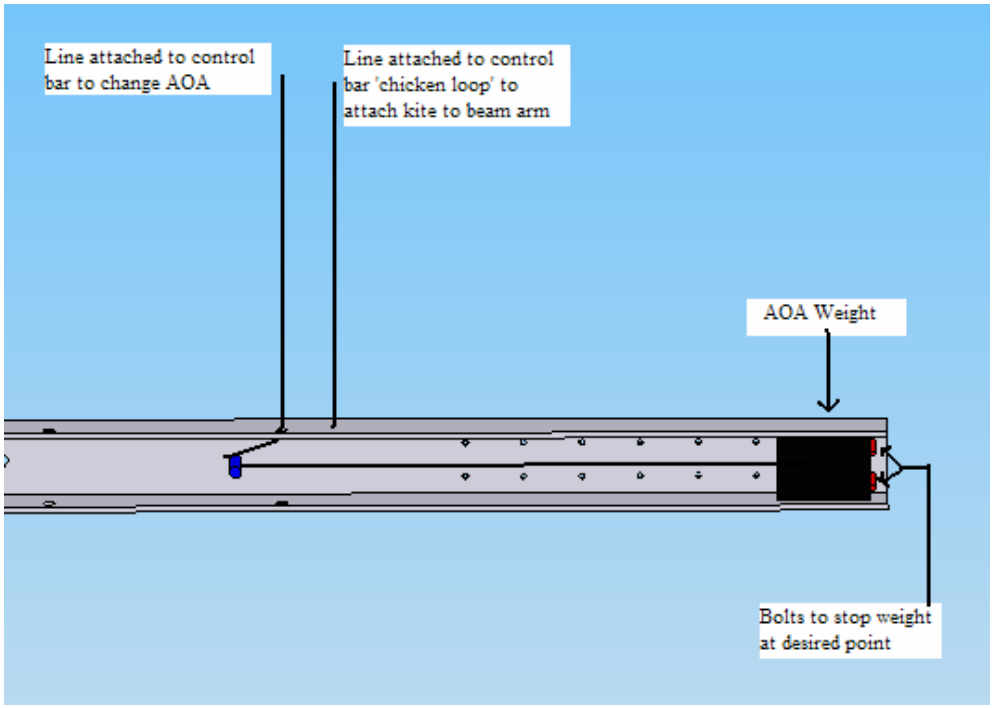

Figure 31 - Exploded View Angle of Attack Mechanism

The two lines extending from the top of the beam arm attach to the kite to connect it to the arm and to allow for the angle of attack to change. The line on the right, as shown in Figure 31, is a stationary line connecting to the 'chicken loop' of the kite control bar. The line to the left is the line that will pull in and let out in order to change the angle of attack of the kite. The left line is attached to the control bar, looped around a smooth bolt, and finally connects to the weight inside the aluminum tube. When the beam is lowered, the weight will slide to the position were the kite is changed to a high angle of attack. This will cause the beam to rise upwards quickly. When the beam reaches the high point in its swing, the weight slides and the kite is put into a low angle of attack. At this point, the retraction springs overcome the force of the kite and pulls the beam back down. When the beam is pulled back down, the kite is placed back into a high angle of attack and the beam rises once again.

The most complicated portion of the structure is the gear system and retraction springs. A close up of this portion of the system can be seen in Figure 32.

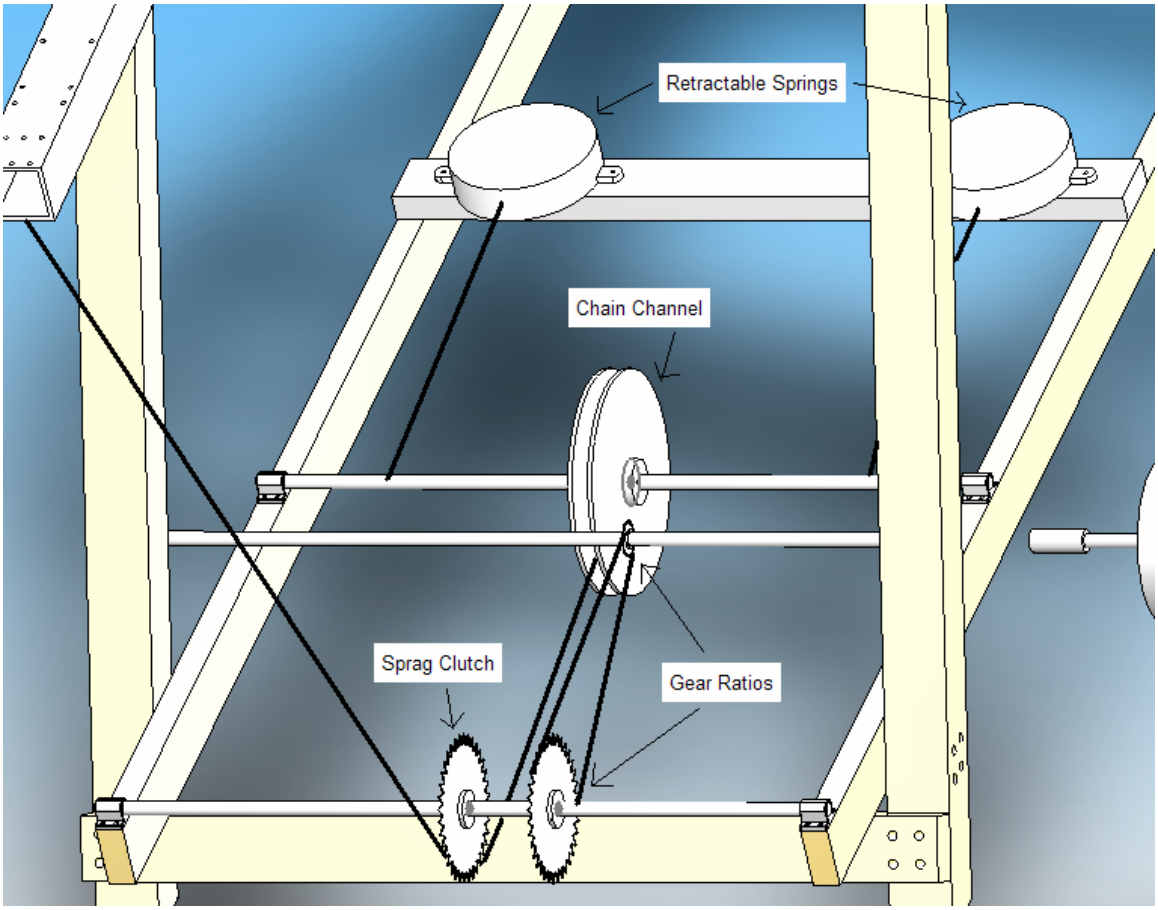

Figure 32 - Exploded View Gear System

As can be seen in this exploded view, the beam will pull on the chain that wraps around the sprag clutch. The chain that wraps around the sprag clutch is then attached to the chain channel. This channel in the pulley will hold the chain that is pulled in as the retraction spring is recoiled. As the chain coils around the center of the pulley it layers on top of itself which allows for a larger amount of chain to be pulled in with the increased radius of the center of the coil. The channel is necessary because the beam pulls out a chain length greater than the capacity of the largest commercial retractable springs available. The gear ratio allows the torque and RPM of the final shaft of the generator to be modified to provide the highest electrical output.

3.2.4 System Construction

The project group did the majority of the construction on the system. The significant sections of the system are as follows: the beam to which the kite will be attached; the gear system needed to turn the generator shaft; the angle of attack mechanism; and the retraction mechanism that will be used to help pull the kite back down to restart the cycle.

Main Wooden Structure

As stated in the previous section, the main structure of the system is a wooden base with a form similar to that of a trebuchet. The base of the structure was constructed with 4”x4” pressure treated lumber for a number of reasons. Lumber is very light in comparison to metals such as steel and the pressure treatment will allow the structure to withstand wet weather conditions. Also, the ease of construction played a major part in the choice to use lumber as the system could be built anywhere with the proper tools and no significant skilled labor, such as welding for steel, would be required.

The system was built with four legs that all stand at a sixty degree angle to the ground for a wide base to maintain stability. Each of the tops of the legs was notched out in order to connect to a horizontal piece of lumber intended to link the front and back together as seen in Figure 33. At the bottom of the sides of the structure, braces were installed in order to keep the legs separated at the desired sixty degree angle. The side braces also have a second purpose as they will be the mounting points for much of the retraction spring and gear systems as depicted in Figure 35.

Figure 33 - Top Side of Structure

Atop the structure are two lengths of lumber that span from side to side. The pieces of lumber are once again 4”x4” stock with notches cut in the undersides at each end in order to link these top pieces to the horizontal pieces spanning from the front legs to the back legs. There are two purposes to these pieces of lumber. First of all they aid in maintaining the stability of the structure when sideways shear forces are impinged on the system. Secondly, these braces will provide a mounting point for the fulcrum point of the beam arm as can been seen in Figure 33 and Figure 34.

Spanning from side to side on the faces of the front and back legs are 2 more sets of braces, as seen in Figure 35. The first pair of braces is attached to the faces of the legs at the bottom of the structure just underneath the braces that span the sides. The second set of front braces are attached approximately three-fourths of the way up the faces of the legs. These two pairs of braces are intended to maintain the rigidity of the structure as well as maintain the desired span between the sides of the structure.

Figure 34 - Structure Braces and Beam Fulcrum Point

Figure 35 - Frontal View of Structure

Turnbuckles

When the main wooden structure was first constructed instability in the structure was observed when a force was applied at the top of the structure from side to side. In order to stiffen the structure a system of turnbuckles were used to apply tension on each side of the structure in an "X" pattern. The turnbuckle assemblies consist of several parts and are as follows:

- 1/8” steel wire
- Steel turnbuckles – open hook / eyelet
- Steel wire loops and clamps
- 3/8” eyelet screws

The eyelet screws were screwed into the faces of the front and back legs just above the bottom braces and below the top braces, as seen in Figure 36, as the main mounting points for the turnbuckle assemblies. The open ends of the turnbuckles were hooked onto the eyelet screws. Steel wire loops were hooked onto the closed end of each of the turnbuckles and the steel wire was threaded from one turnbuckle to the opposing turnbuckle to form the desired “X” pattern. Once the steel wire was threaded the clamps were attached to the wire to secure the wire in place and the turnbuckles were tightened to apply the desired tension on the structure. With the addition of the turnbuckles, the structure became a completely rigid structure when considering an applied side – to – side force.

Figure 36 - Turnbuckle Assembly

Balanced Arm Assembly

In the final design of the kite power demonstrator the kite will attach to the top of the beam at the top of the structure. In order to maximize the number of different testing setups, the balanced beam was designed with two main features. First, the beam is constructed of two different sizes of aluminum square tubing in order to allow for telescoping of the smaller tube inside the large tube. The beam consists of two square aluminum tubes with outer diameter of 3.5" at a length of 5' each and a third length with an inner diameter of 3.615" and a length of 8'. Second, a series of holes was drilled in the sides, top, and bottom of the 3 lengths of aluminum tubing in order to secure the lengths of aluminum at any desired length for testing purposes. These length changes will allow for changes in weight and beam length from the front of the structure to the back.

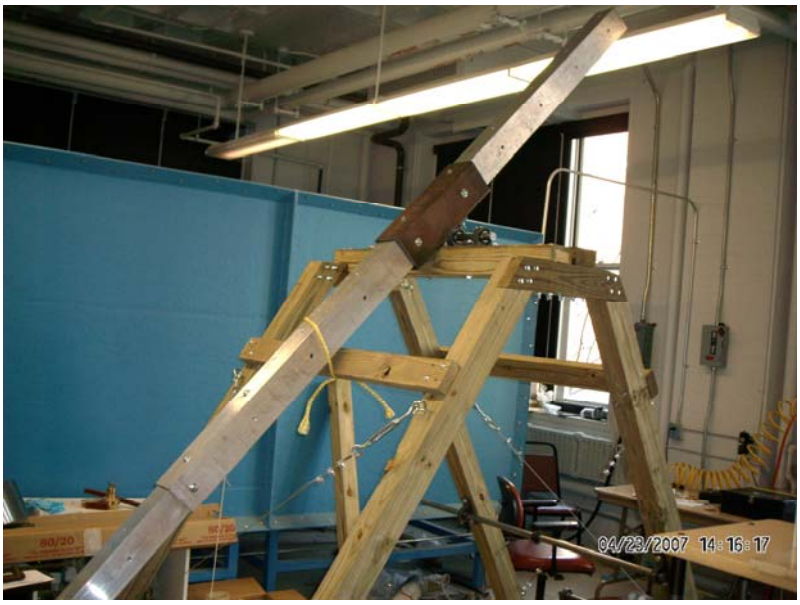

Figure 37 - Balanced Arm Assembly

Fulcrum Point Assembly

The fulcrum point is the attachment point at the top of the wooden structure for the aluminum beam. In order to enhance the ability of the beam to change in length, as discussed above, the beam is set inside another square tube with holes drilled into it in the same fashion as the beam. Therefore, the beam can now attach at the fulcrum point with bolts in different holes. The steel square tube has an outer diameter of 5" and in inner diameter of 4.5". There is a significant amount of variance between the outer diameter of the large aluminum tube (4") and the inner diameter of the steel tube in order to have the ability to thread bolts down through the bottom of the steel tube.

The bolts that were threaded through the bottom of the steel tube are attached to two pillow block bearings with an inner bearing diameter of 1". On top of the structure there are an additional two pillow blocks mounted to the top wooden braces spanning the structure. These two additional pillow blocks make up the second half of the rotating fulcrum point with the addition of a 1" diameter steel rod. The steel rod is threaded through the four pillow blocks to form the axle for the fulcrum point. Figure 38 shows the fully assembled fulcrum point.

Figure 38 - Beam fulcrum point assembly

Angle of Attack Change Mechanism Assembly

One of the most essential features of the kite power demonstrator is the assembly of the angle of attack change mechanism. When determining which system design would work best for this project one key consideration was the ability to incorporate a mechanism to change the angle of attack of the kite. In the final design of the system the angle of attack change mechanism was incorporated into the balanced beam arm described above.

To limit the complexity of the system it was essential to design a very novel AOA change mechanism. The final design incorporates the inner square tube at the front of the demonstrator and a simple weight system. As shown in Figure 39, there is a series of holes drilled through the sides of the small aluminum tube. These drilled holes are intended to hold two bolts, which are currently inserted into the holes at the very far right of the arm, with the purpose of stopping the sliding weight of the mechanism. A range of holes was drilled in order to apply another level of testing in the system design. The current design enables the bolts that stop the weight to be either ahead of or behind the kite attachment point.

The attachment point for the kite is the eyelet bolt located on the arm in the left side of Figure 39. This bolt will be utilized by attaching a carabineer to the closed loop of the bolt and then attaching the ‘chicken loop’ of the kite control bar to the carabineer. This setup will attach the kite to the beam arm in order to lift it during motion. The bolt, only hex nut visible, to the left of the eyelet bolt is the point around which the line from the weight to the control bar will pass as it is pulled through a hole in the top of the beam

arm. Rather than using a pulley deep inside the beam arm it was believed to be a more novel design to simply use a bolt with a smooth surface as the turning point for the line.

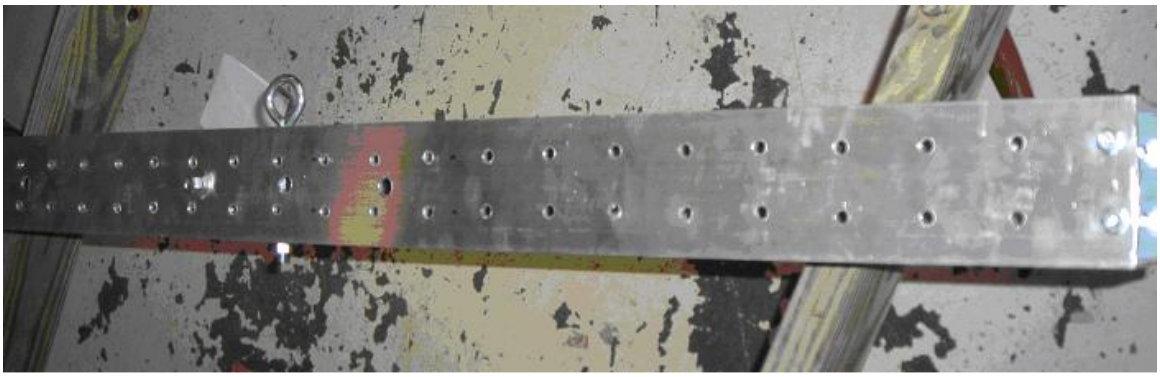

Figure 39 - Angle of Attack Change Mechanism Assembly

Axles / Gears Assembly

The portion of the system intended to convert the linear motion into a rotary motion consists of a series of axles and gears as shown in Figure 32. The gear assembly consists of two steel axles of 1" diameter, two 9.2" sprockets, one 2.3" sprocket, and four pillow block bearings. At the front of the system the main axle is mounted with two pillow blocks attached to the wooden side brace that extends out from the front of the structure. On this axle, the two large sprockets are mounted. As viewed in Figure 40, the left large sprocket is intended to be used with the retraction mechanism and the right sprocket is part of a 'gearbox' system. The axle mounted to the back of the front structure legs is the second half of the 'gearbox' system. This axle is also mounted on two pillow blocks and holds the small sprocket. In order to turn the small sprocket a chain will be looped around both the large and small sprockets. The ratio in sizes from the large

sprocket to the small sprocket will allow for a greater number of rotations of the small sprocket, increasing the rpm value and thus the potential power output.

The third axle shown in Figure 40, resting on the brace in front of the mounted sprockets, is intended for use with the retraction spring system. This axle would also be mounted with two pillow blocks, but this mechanism has not been completely designed and will require future work.

Figure 40 - Axles and Gears Assembly

3.3 System Simulations

The ultimate goal of mechanism simulation is to predict the kite motion and the power generated by the mechanism. The two major figures of interest are the RPM of the shaft and the Torque it is experiencing. Once initial estimates of these quantities are found, it then will then be possible to manipulate the simulations to find the most efficient design of the system. From these most efficient designs we can also predict the eventual power producing capabilities of our mechanism. Simulations for the system

were based on both steady state simulations and dynamic model involving differential equations.

3.3.1 Steady State Simulations

The steady state kite modeling we conducted is based upon previous work. Some important variables are defined in Figure 41:

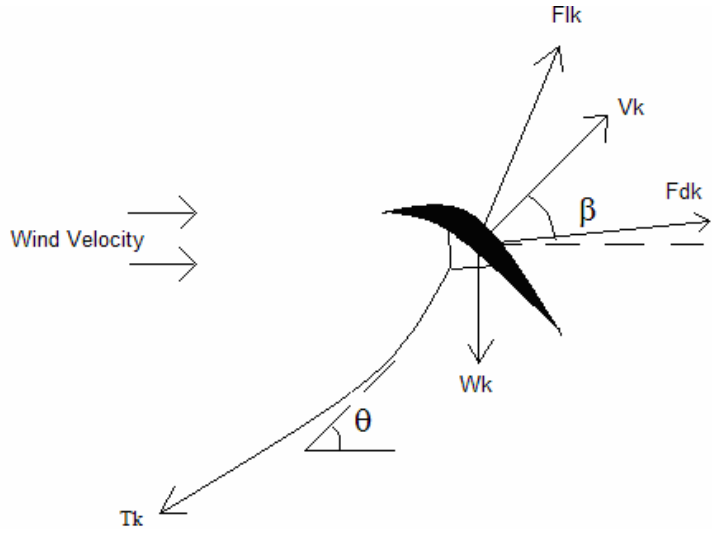

Figure 41 - Kite Model, From Goela (1983)

Goela's steady state analysis is coupled to a model of the oscillating arm in our demonstrator. In addition, a new aerodynamic model is incorporated to better model the kite behavior. The derivation of the entire model begins with the motion of the kite. Variables used in the steady state kite calculations are:

V = Wind Velocity	*Wk = Weight of the Kite*
β = Angle of Kite motion relative to ground	*Ak = Area of Kite*
Vk = Velocity of kite from arm Movement	*ρ = Density of air*
Flk = Force of lift on the Kite	*g = Gravity constant*
θ = Angle of Kite with respect to ground	*α = Kite's assumed angle of attack*
Tk = Line Tension	*AR = Kite Aspect Ratio*
Fdk = Force of drag on the kite	*eo = Assumed Value for Drag Calculation*
Cdo = Assumed Drag Coeffcient	

The goal of the steady state kite calculations is to find the kite tether tension created by the kite. From Goela (1986), it was shown that the normalized kite velocity, normalized kite weight, and the lift over drag ratios are required to develop an equation for the kite tether tension.

The first step towards the normalized kite velocity is determining the velocity of the kite given by:

$$Vwr = \sqrt{V^2 + Vk^2 - 2 \cdot V \cdot Vk \cdot \cos(\beta)} \quad \textbf{(4)}$$

Where the Velocity of the Kite from arm motion is calculated using:

$$Vk = \frac{Ra \cdot \omega}{\cos\left(\gamma - \beta + \frac{\pi}{2}\right)} \quad \textbf{(5)}$$

Two of these terms come from the design of the Mechanism:

Ra = Length from Pivot Point to Kite Tether ω *= Angular Velocity of Rotataing Arm*

γ *= Angle between Arm and ground level*

With the total kite velocity we can then find a value for the kite Normalized Velocity:

$$Vwrnorm = \frac{Vwr}{V} \quad \textbf{(6)}$$

For the lift over drag coefficients, equations modeling the aerodynamic performance of airfoils were added to Goela's (1983) steady state analysis. This aerodynamic model replaced the L/D values used in Goela (1983). A range of angles of attack were simulated through the use of Lift over Drag ratios that simulate the kite at various angles of attack. This range of L/D values can be determined from basic airfoil theory and finite wing theory. Using this theory we can approximate values of Cl and Cd that define L/D. The Coefficient of Lift (Cl) is found using basic airfoil theory:

$$Cl = \left(\frac{d}{d\alpha} Cl\right) \cdot \left(\alpha - \alpha_{ZeroLift}\right) \quad \textbf{(7)}$$

Using finite wing theory the derivative of the coefficient of lift is assumed to equal:

$$\frac{d}{d\alpha} Cl = \frac{2 \cdot \pi}{1 + \frac{2 \cdot \pi}{\pi \cdot AR}} \quad \textbf{(8)}$$

Substituting equation **(8)** into Equation **(7)** gives the coefficient of lift:

$$Cl = \frac{2 \cdot \pi \cdot \alpha}{1 + \frac{2}{AR}} \quad \textbf{(9)}$$

The coefficient of drag (Cd) is found by:

$$Cd = Cdo + \frac{Cl^2}{\pi \cdot AR \cdot eo} \quad \textbf{(10)}$$

Using the calculated values of Cl and Cd we can find a range of Lift over Drag ratios with:

$$\frac{L}{D} = \frac{Cl}{Cd} \quad \textbf{(11)}$$

The inverse of Lift over Drag is simply:

$$\frac{D}{L} = \frac{1}{\frac{L}{D}} \quad \textbf{(12)}$$

Equations **(11)** and **(12)** represent Lift over drag and drag over lift coefficients that are functions of the kite's angle of attack (α). The last step is to find values for normalized kite weight:

$$Wknorm = \frac{Wk \cdot g}{0.5 \cdot \rho \cdot V^2 \cdot Cl \cdot Ak} \qquad \textbf{(13)}$$

Finally, from Goela (1983) the calculation of a line Tension Normalized coefficient is found:

$$TL = \sqrt{Vwrnorm^4 \cdot \left[\left(\frac{D}{L}\right)^2 + 1\right] + Wknorm^2 - 2 \cdot Wknorm \cdot Vwrnorm \cdot \left[1 - Vr \cdot \cos(\beta) - \left(\frac{D}{L}\right) \cdot Vr \cdot \sin(\beta)\right]}$$

(14)

From this normalized equation we can find numerical tension values:

$$T = TL \cdot 0.5 \cdot \rho \cdot V^2 \cdot Cl \cdot Ak \qquad \textbf{(15)}$$

Using the line tension a formula can be found to determine the power harnessed by the oscillating beam in the form:

$$P = TL \cdot \cos(\gamma) \cdot Rc \cdot \omega \qquad \textbf{(16)}$$

Using the Line tension from the steady state kite model, we can estimate the forces acting upon our mechanism design. Additional parameters used to model the oscillating beam design were included. Steady state equations for the mechanism were based on the model seen in the following figure:

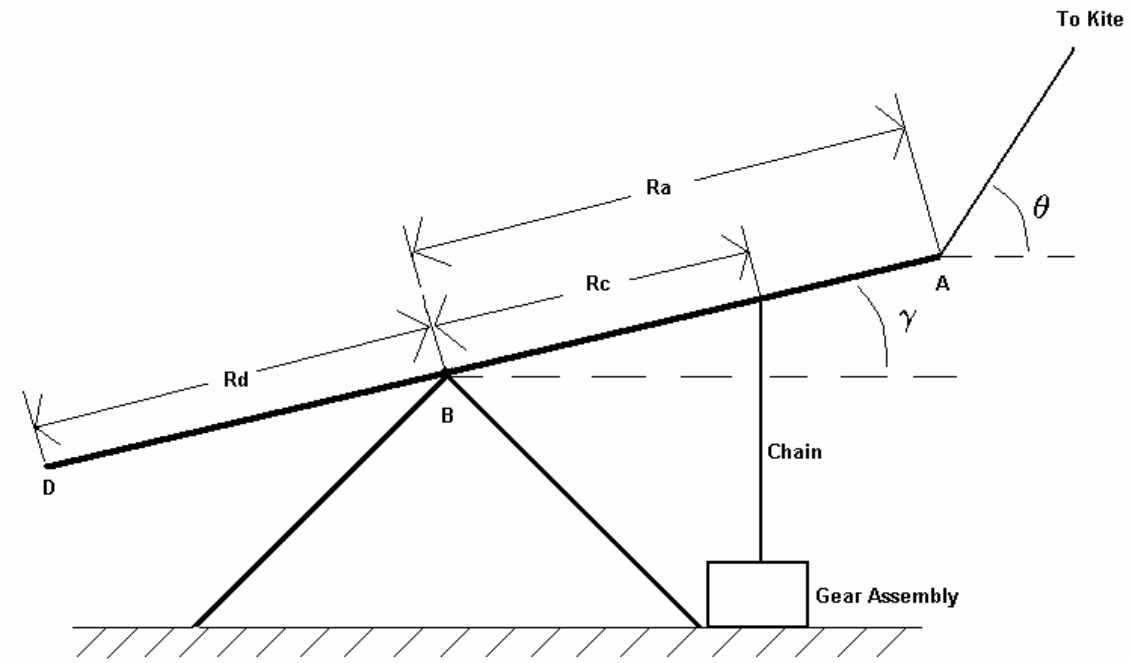

Figure 42 - Pivoting Arm Diagram

Variables for the pivoting arm simulation:

Ra = Length from Point A to Point B	*θ = Angle of Kite with respect to ground*
Rc = Length Arm from Point B to Chain	*β = Angle of Kite motion relative to ground*
Rd = Length Arm from Point D to Point B	*ω = Angular Velocity of Rotataing Arm*
W_DB = Arm Weight between D and A	*γ = Angle between Arm and ground level*
W_BA = Arm Weight between B and A	*Tk = Line Tension from Kite*
W2 = Weight of Angle of Attack Weight	*Tc = Tansion on chain*

With the line tension calculated from steady state theory, it is possible to sum moment's about the rotating arm's pivot point to calculate the tension that would be created on the chain going into the gear system, as follows:

$$Tc \cdot \cos\left(\gamma - \theta + \frac{\pi}{2}\right) \cdot Ra - Tc \cdot \cos(\gamma) \cdot Rc + W\_DB \cdot \cos(\gamma) \cdot \frac{Rd}{2} - W\_BA \cdot \cos(\gamma) \cdot \frac{Ra}{2} - W2 \cdot \cos(\gamma) \cdot R2 = 0$$

(17)

Solving for the Chain tension yields:

$$Tc = \frac{T2 \cdot \cos\left(\gamma - \theta + \frac{\pi}{2}\right) \cdot Ra + \left(g \cdot W\_DB \cdot \cos(\gamma) \cdot \frac{Rd}{2} - g \cdot W\_BA \cdot \cos(\gamma) \cdot \frac{Ra}{2} - W2 \cdot \cos(\gamma) \cdot R2 \cdot g\right)}{\cos(\gamma) \cdot Rc} = 0$$

(18)

Using calculated values for the kite line tension, the chain tension can now be determined. The next step is then to use this chain tension to estimate Torque and rotational speed of a generator shaft. A simple gear system shown in the Figure 43:

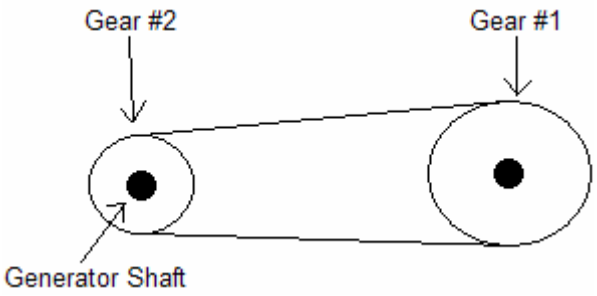

Figure 43 - Two Gear-System Schematic

In the gear system shown above, the chain attached to the pivoting beam is spinning the shaft on gear #1, and is giving Gear #1 a given torque and RPM value. The following values are defined for the gear system:

St = Stroke Time
Sl = Stroke Length
r1 = radius of first gear
T4 = Torque on Generator Shaft
RPM2 = Rotational speed of Gear 2
Q1 = Number of gear teeth for first gear
Q3 = Number of gear teeth for second gear
r2 = radius of second gear
RPM1 = Rotantioanl speed of Gear 1

Torque on a given gear is usually approximated by multiplying the chain tension and the radius of the gear or the gear ratio of the gearbox in use. From this approximation we can find the torque on the generator shaft using the following equation:

$$T4 = Tc \cdot r2 \qquad \textbf{(19)}$$

The predicted RPM of the generator shaft depends Stroke time of the rotating arm, which is approximated by finding the time required for a kite to travel through its power phase. The RPM of Gear #1 and Gear #2 are found using:

$$RPM1 = \frac{\frac{Sl \cdot 60}{St}}{2 \cdot \pi \cdot r1} \quad \textbf{(20)}$$

Using the value of this rpm we can estimate the RPM this would create on the connected Gear #2:

$$RPM2 = \left(\frac{Q1}{Q3}\right) \cdot RPM1 \quad \textbf{(21)}$$

This is the final step in our steady state theory. Results from the steady state theory model will be given in a later section.

3.3.2 Dynamic Modeling Simulation

Dynamic simulations of the system provide a much deeper look at the possible power production and overall operation of the entire mechanism. This simulation allows the operational characteristics of the system to be viewed in response to time. It also allows for average values of system production that can be used to determine valuable information. The major advantage of this system over the steady state theory is that it allows predictions on the functionality of the system. The system will have the ability to predict whether a given mechanism setup will be able to run effectively or autonomously.

For the dynamic modeling, the simulation was created to model a slightly modified version of the mechanism. This slightly modified version of the system included a load on one end of the bar to replace the downward pull of the retraction

spring. This was created due to worries that a retractable spring would not be found in time for the systems construction. Therefore the system was simulated as if our project team needed an extra load to prove the concept that the pivoting beam could continually rock in an up and down movement. A diagram of the modified mechanism is shown here:

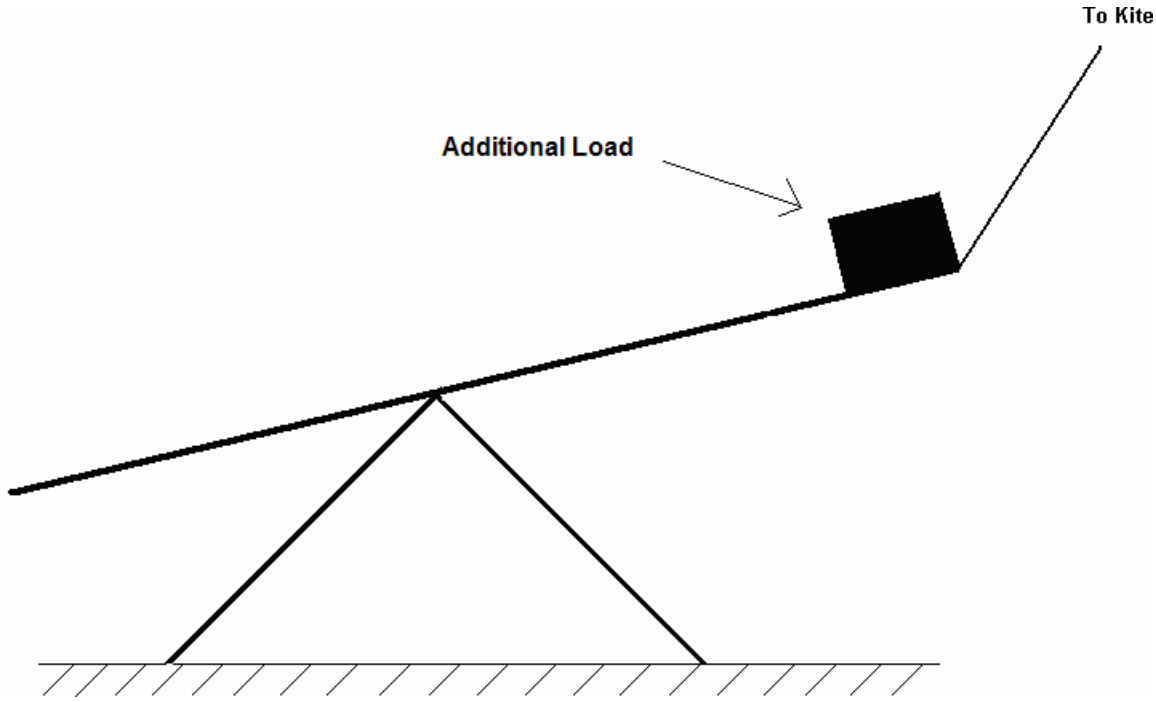

Figure 44 - Modified System Simulation

One difference with this simulation is that the overall power of the system will be based off of the mechanical power generated by the rotating arm. This power is approximated using:

$$P = T \cdot \omega \quad \textbf{(22)}$$

Where:

T = Torque of Rotating Beam ω = Rotational Speed of Rotating Beam

The mathematical equations used for this dynamic simulation begin with kite dynamics found in Dr. Goela's equations. Using Figure 45, two coordinates are defined:

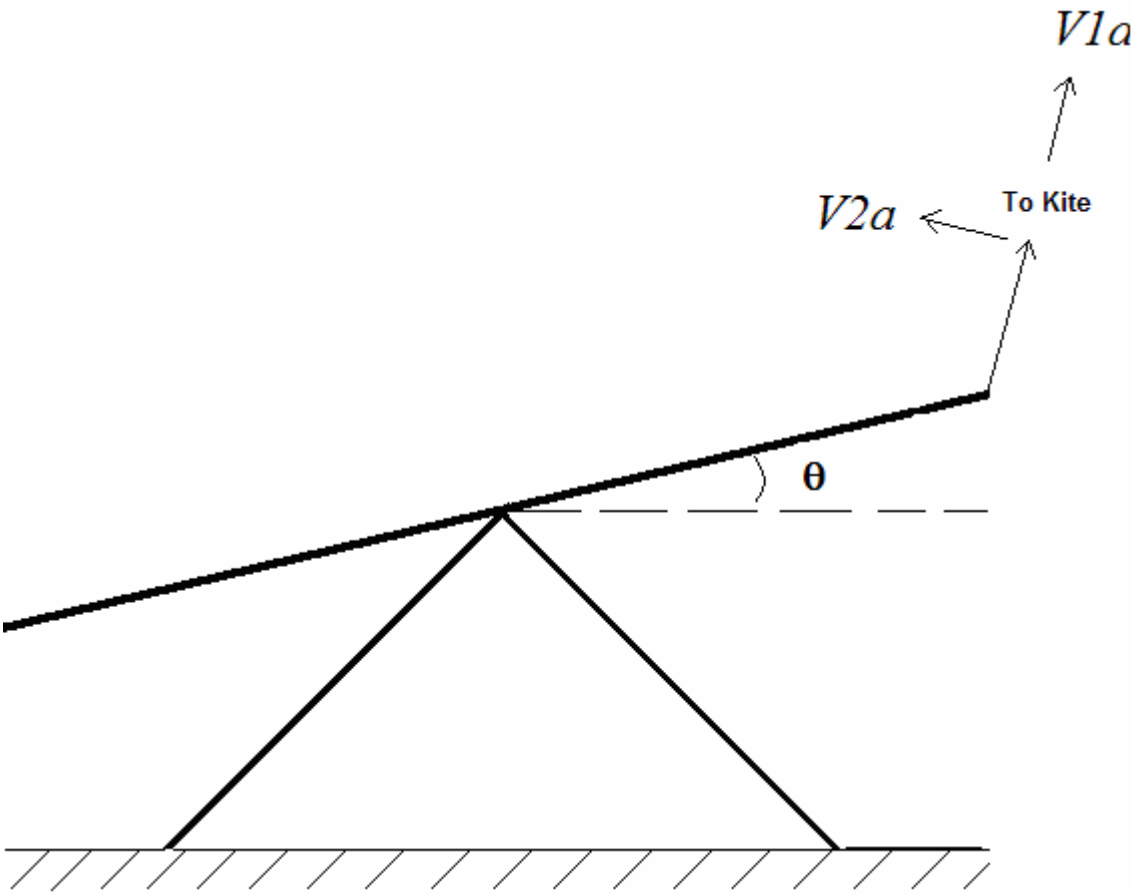

Figure 45 - Simulation Parameters

In this figure V1a represents the velocity of the kite in the tether line direction while V2a represents the kite velocity perpendicular to the kite tether direction. From Goela (1986), we find an equation for the change in velocity in the V2a direction:

$$\frac{d}{dt}V2a = \left(\frac{g}{wk}\right)\cdot\left(F\_dk\cdot sin(\theta+\phi) - F\_lk\cdot cos(\theta+\phi) + Wk\cdot cos(\theta) + \frac{2\cdot Wk\cdot V1a\cdot V2a}{g\cdot L1}\right)$$

(23)

Where the end term is the coriollis force based on a variable tether line length used in the Goela (1986) report:

$$Coriolis\ \ Force = \frac{2\cdot Wk\cdot V1a\cdot V2a}{g\cdot L1} \qquad \textbf{(24)}$$

The sprag pump has no variation in the tether line length. Since the kite is attached to the beam it is obvious that there is no velocity or movement towards the V1a direction. Therefore the coriollis force can be ignored because the velocity in the V1a direction is:

$$V1a = 0 \qquad \frac{d}{dt} V1a = 0 \qquad \textbf{(25)}$$

Therefore the change in velocity of the kite in the V2a direction is:

$$\frac{d}{dt} V2a := \left(\frac{g}{wk}\right) \cdot \left(F\_dk \cdot \sin(\theta + \phi) - F\_lk \cdot \cos(\theta + \phi) + Wk \cdot \cos(\theta)\right) \qquad \textbf{(26)}$$

Looking in the V1a direction it is found from Goela (1986) that the change in the kite's velocity is assumed to be:

$$\frac{d}{dt} V1a = \left(\frac{g}{wk}\right) \cdot \left(F\_dk \cdot \sin(\theta + \phi) - F\_lk \cdot \cos(\theta + \phi) + Wk \cdot \cos(\theta) + \frac{2 \cdot Wk \cdot V1a \cdot V2a}{g \cdot L1}\right) + \left(Wk \cdot \frac{V2a^2}{g \cdot L1}\right) - Ft$$

(27)

Since the V1a derivative is known to have a value equal to zero, the equation can be rearranged to solve for the kite tension. The kite tension is now found as:

$$Ft = Fdk \cdot \cos(\theta + \phi) + Flk \cdot \sin(\theta + \phi) - Wk \cdot \sin(\theta) + Wk \cdot \frac{V2a^2}{g \cdot L1} \qquad \textbf{(28)}$$

Using the equations already mentioned the dynamics of the kite can be simulated based on a given set of initial conditions for the kite. The next step is to couple the kite dynamics into the oscillating motion of the arm. The change in the angle theta is calculated based upon the movement of the kite's velocity. The velocity in the V2a direction shows:

$$-V2a = \dot{\theta} \cdot L1 \qquad \textbf{(29)}$$

This can be rearranged to express:

$$\frac{d}{dt}\theta = \frac{-V2a}{L1} \quad \textbf{(30)}$$

Further calculations coupling the kite motion and the oscillating arm can are found using another figure:

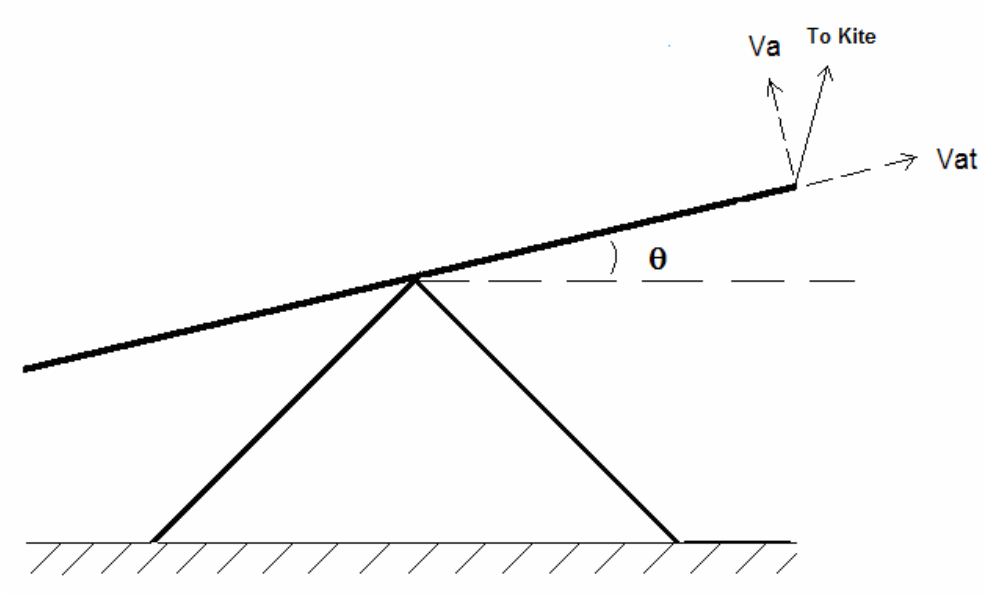

Figure 46 - Simulation Parameters Part #2

In this figure, Va represents the velocity of the beam perpendicular to the beam while Vat represents the velocity of the beam parallel to the beams orientation. In this case the sum of the moments about the rotating beam culminates in the following equation:

$$\frac{-1}{g}\cdot\left(Wda + I\_AD\cdot\frac{g}{RA}\right)\cdot\left(\frac{d}{dt}Va\right) - \left(\frac{2}{g}\right)\cdot\left(W\_DA + I\_AD\cdot\frac{g}{LL^2}\right)Vat\cdot\frac{Va}{LL} = Ft\cdot\cos\left(\gamma - \theta + \frac{\pi}{2}\right)\cdot RA - Fc\cdot\cos(\gamma)\cdot Rc$$

(31)

In this case it is very obvious that the beam does not have any motion in the Vat direction because of the beam arm is fixed in a rotating form. Therefore it can be assumed that:

$$Vat = 0$$

The velocity in the Va direction can be calculated from:

$$Va := RA \cdot \omega \quad \textbf{(32)}$$

Where the angular velocity of the beam is:

$$\omega := \frac{d}{dt}\gamma \quad \textbf{(33)}$$

Hence, the following equation if found:

$$\frac{d}{dt}\gamma := \frac{Va}{RA} \quad \textbf{(34)}$$

The power of the mechanical system is calculated based on the power of the rotating beam. This is calculated by:

$$P = T \cdot \omega \quad \textbf{(35)}$$

Substituting for the angular velocity we find that the power is:

$$P := T \cdot \frac{Va}{RA} \quad \textbf{(36)}$$

The main key to the simulations lie in the four differential equations **(23), (30), (31), and (34)**. Using these four equations and setting some initial quantities allows for the determination of the kite and oscillating beam dynamics. With Matlab, a given time step is used to determine the number of iterations involved in the differential equations. Once initial quantities are set, the Matlab program runs the coupled equations over a set time limit to simulate the system dynamics.

One problem with these equations is that they do not involve the use of the angle of attack mechanism. They only describe the beam and kite motion as it moves in one direction, either up or down. Therefore, Matlab is set to a point that when the oscillating

beam reaches a given height, the kite's angle of attack is altered. When the beam reached a given angle with the horizontal field, the code changes the kite's angle of attack to respond to the changing beam angle with the horizontal. For example, when the rotating mathematically reaches a given downward angle with the horizontal, the kite's angle of attack is changed to a higher set value that triggers the kite to provide a force. An example is shown here:

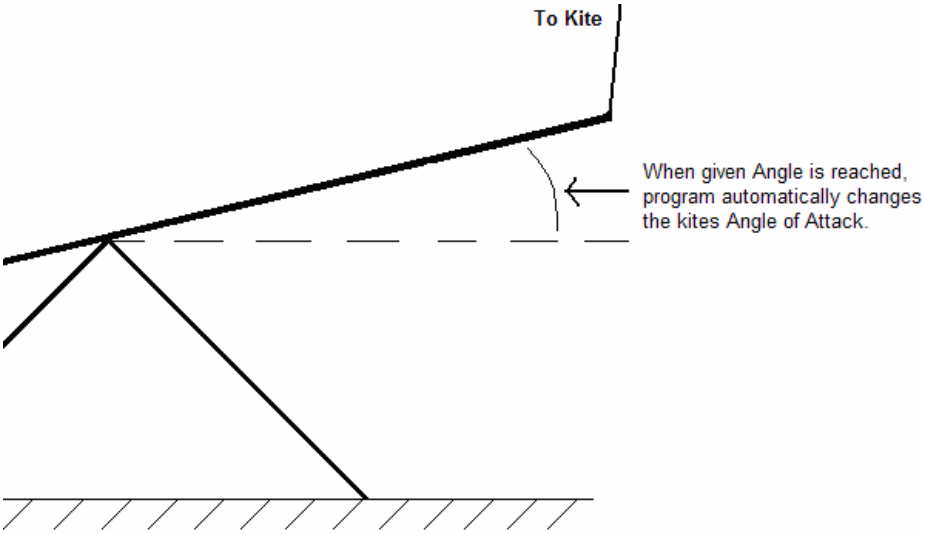

Figure 47 - Rotating Beam reaches a set Angle in the program

Results from this dynamic model simulation are given in a later section.

3.4 System Stress Analysis

Stress calculations for the Sprag Combo demonstrator begin with the analysis of the long pivoting beam. The concern is whether the beam can withstand the full force of the kite pulling on one end of the beam. The stress calculations for the beam are based on the equation of a beam fixed at one end with a load placed at the free end.

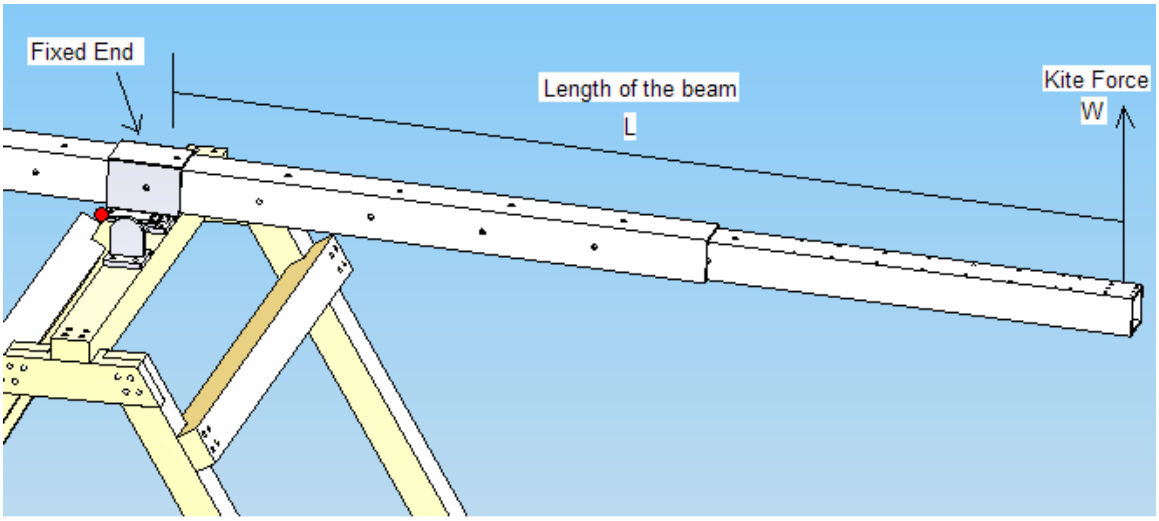

Figure 48 - Beam Stress

The highest stress that the beam will be placed under is at the fixed end support of the beam. The stress at this point can be calculated from the equation:

$$Stress := W \cdot \frac{L}{Z} \qquad (37)$$

Where the terms in this equation are identified as:

W = Kite Force
L = Length of the beam
Z = Beam Section Modulus

The beam section modulus is found by analyzing the cross section of the beam:

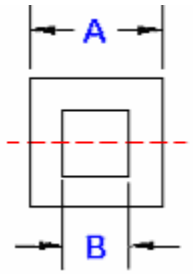

Moment of Inertia

$$I = \frac{\left(A^4 - B^4\right)}{12} \qquad (38)$$

Section Modulus

$$Z = 2 \cdot \frac{I}{A} \qquad (39)$$

The other concern with the beam is its deflection. The largest deflection that the beam will undergo is at the free end where the kite force is located. This maximum deflection is found using the equation:

$$\text{Deflection} := W \cdot \frac{L^3}{3 \cdot E \cdot I} \quad \textbf{(40)}$$

The new term introduced in this equation is the Elasticity Module (E) that is determined by the beam material. The next analyzed component of the system is the center beam on which the pivot rests (Figure 49).

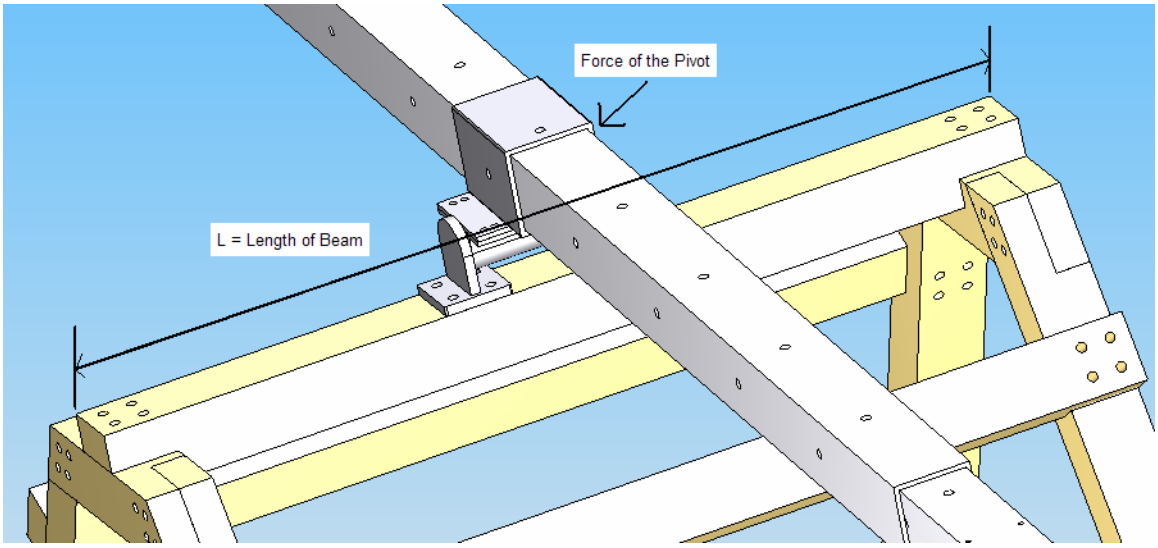

Figure 49 - Top Support Beam

The beam can be shown as a beam supported at two ends with a downward force in the middle. A body force diagram shows:

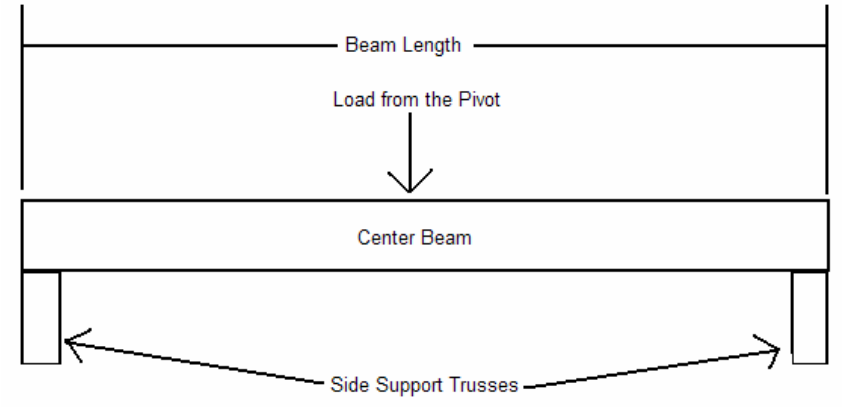

Figure 50 - Beam Stress Diagram

From this type of load on the beam the stress at the center of the constant cross section is determined from the equation:

$$\text{Stress} := W \cdot \frac{L}{(4 \cdot Z)} \quad \textbf{(41)}$$

The maximum deflection of the center beam is at the center of the beam at the pivots location and is calculated using:

$$\text{Deflection} := W \cdot \frac{L^3}{48 \cdot E \cdot I} \quad \textbf{(42)}$$

These components represent the major concern for the stress analysis of our structure.

4. Results

Results come directly from the equations and details explained in our methodology section. They are divided into three separate sections. The first of these sections is the data collected from physical testing of the kite systems. The second and third sections are the numerical predictions of the model simulations and the possible stresses that the model simulation predictions will create on our mechanical system.

4.1 Kite Testing

Several trips were made to the local sport kite shop, PowerLine Sports in Seabrook, NH, where three kites were tested. Two of these kites were demonstration kites that were tested using our digital tension meter setup. The first of these kites was the Ozone Axis 4 m^2. The kite and its characteristics are listed below:

Figure 51 - Ozone Access 4m

Kite Area (m^2)	2 m^2
Kite Weight (Kg)	1 lb. 5 oz.
Kite Length	135 (in.)

Middle Width	46 (in.)
Tip Width	30 (in.)
# of Control Lines	Four
Minimum Required Wind Speed (m/s)	3 m/s

Table 4 - Ozone Axis Kit Characteristics

Using this kite the following data was collected:

	Average Wind Speed (mph)	Angle of Attack (deg.)	Tension Reading (lb)	Coefficients of Lift
De-Powered				
	avg. 10.5 mph	avg. 70-74	4	0.33
			7	0.58
			8	0.66
			11	0.90
			13	1.07
			Avg 0-11	
Powered				
	avg. 10.5 mph	80	7	0.575743118
		80	4	0.328996067
		85	11	0.904739185
		70	20	1.644980336
		60	20	1.644980336
		avg. 70-80	avg. 12-20	

Table 5 - Ozone Axis Tension Data

From our data collection, an assessment for the kite's coefficient of lift data was created.

From the data, at assumed zero angle attack the average Cl was:

$$Cl = \frac{22.24}{.5 \cdot 1.225 \cdot 4.7^2 \cdot 4}$$

$$Cl = 0.411$$

At α = 18 degrees the average lift was 16 lb. resulting in a Cl of:

$$Cl = \frac{71.17}{0.5 \cdot 1.225 \cdot 4.7^2 \cdot 4}$$

$$Cl = 1.315$$

Since the coefficient of lift vs. Angle of attack is linear we can approximate the slope of the line between α = 0 and α = 18. This slope was found to be:

$$Cl\ Slope = 0.0486$$

Hence an approximate equation for the kite's coefficient of lift as a function of angle of attack:

$$CL := (0.0486) \cdot \alpha + 0.057 \qquad \textbf{(43)}$$

The second kite tested was the 7 m^2 Cabrinha Crossbow. For this kite, the kite line tension was measured along with the force required to move the Power/De-power bar. The force on the Power/De-Power bar is important because it gives an idea for the size or size of a counterweight or spring mechanism. The Cabrinha kite and its characteristics are detailed below:

Figure 52 - Cabrinha Crossbow 7m

Kite Area (m^2)	7 m^2
Kite Weight (Kg)	5 lb. 4 oz.
Kite Length	215 (in.)
Middle Width	55 (in.)

Last strut Width	38 (in.)
# of Control Lines	Four
Minimum Required Wind Speed (m/s)	3 m/s

Table 6 - Cabrihna Cross Kite Characteristics

The Cabrihna Crossbow is an LEI kite. The inflatable edge and inflatable struts are filled with air that is pumped into the kite through a hand air pump. For this kite the digital tension meter setup was also used and the following data was collected:

	Average Wind Speed (mph)	Angle of Attack (deg.)	Tension Reading (lb)	Coefficients of Lift
Depowered				
	avg. 13.5 mph	avg. 79-85	Avg. 0-4	0.05686621
Powered				
	avg. 13.5 mph	avg. 79-85	42	1.194190408
			28	0.796126939
			22	0.625528309
			24	0.682394519
			23	0.653961414
			22	0.625528309
			16	0.454929679
			10	0.28433105
			12	0.341197259
			38	1.080457988
			23	0.653961414
			16	0.454929679
			18	0.511795889
			21	0.597095204
			24	0.682394519
			22	0.625528309
			18	0.511795889
			35	0.995158674
			20	0.568662099
			mostly stayed at 23	0.653961414

Table 7 - Collected Data for Cabrihna Crossbow 7 m^2

The angle of attack is approximated in these calculations in the same way that it was approximated in the calculations for the Ozone Axis. At assumed zero angle of attack the average Cl was:

$$Cl = \frac{8.9}{0.5 \cdot 1.225 \cdot 6.035^2 \cdot 7}$$

$$Cl = 0.057$$

At α=8 deg. the average lift was 23 lb. resulting in a Cl of:

$$Cl = \frac{102.31}{0.5 \cdot 1.225 \cdot 6.035^2 \cdot 7}$$

$$Cl = 0.655$$

The slope of the line between α=0 and α=8 is found to be:

$$Cl\ Slope = \frac{0.655 - 0.057}{8}$$

$$Cl\ Slope = 0.075$$

An equation can be found for the coefficient of lift as a function of Angle of Attack:

$$CL = (0.075) \cdot \alpha + 0.057 \qquad \textbf{(44)}$$

Additionally, the force required on the Power/de-power bar was measured to vary from 0-10 lb., with the force becoming greater as the bar was moved into the powered position.

The third and final kite tested was the Peter Lynn Guerilla that was purchased as part of the project. The kite was larger then the other two previously tested kites, and it was calculated that the kite would pull with a force greater then the capability of the tension meter. Therefore, we used a spring to determine the spring tension. The spring used was a large industrial spring found in Washburn Laboratories.

The first step in using the spring was finding its calibration curve so that we could determine the length that the string stretches for a given force. In our laboratory, the spring's extension was measured for a variety of different weights. The data taken is seen here:

Weight (N)	Spring Extension (in.)
145.7375	0.625
179.66875	1.0625
282.01875	2.375
348.76875	3.25
460.01875	4.875
571.26875	7

A graph of the data should represent a linear line to represent a spring deflection vs. a load. Plotting the data shows:

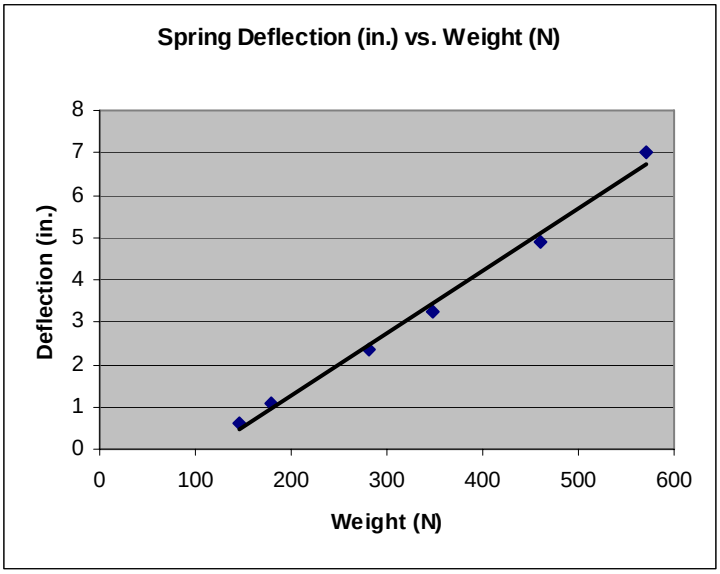

Figure 53 - Spring Deflection vs. Weight (N)

Using this chart the deflection of the spring was measured with the movement of the kite. This spring method testing our kite was attempted once but due to bad weather conditions at the time of testing, unreliable results were obtained.

4.2 Determination of Simulation Values

From the data acquired from our beach testing, and the known values concerning our kite, it is possible to make predictions based on the steady state theory, pivoting arm, and RPM/Torque based on the simulation models.

4.2.1 Steady Sate Simulation Results

Beginning with the steady state kite theory, the known and assumed values are determined. The following values are known:

$V = 5$ m/s	Wind Velocity	$Wk = 2.38$ kg	Kite Weight
$Ak = 10$ m^2	Kite Area	$AR = 5$	Kite Aspect Ratio
$g = 9.81$ m/s^2	Gravity	$\rho = 1.167$ kg/m^3	Air Density
$\gamma = 20$ degrees	Angle of arm rotation	$Ra = 2.4384$ m	Length from pivot to tether

From direct observations it has been determined that the approximate value can be assumed for the kite motion:

$\beta = 135$ degrees Kite Angle Motion

The rotational speed of the oscillating arm is approximated based upon a reasonable estimation:

$$\omega := \frac{1.0}{s} \quad \text{Rotating arm angular velocity rad/s}$$

Using the known and unknown values, the first calculation is the velocity of the kite due to the arm motion. From equation **(5)**, this value is calculated:

$$Vk = 2.61 \frac{m}{s}$$

Then using equation **(4)**, the velocity of the kite is:

$$Vwr = 7.09 \frac{m}{s}$$

The normalized velocity of the kite is:

$$Vwrnorm = 1.418$$

With this in mind, the coefficients of lift and the corresponding normal weight of the kite values are made to be functions of a range of angles of attack. Using these values the tether line tension is calculated as a function of angle of attack:

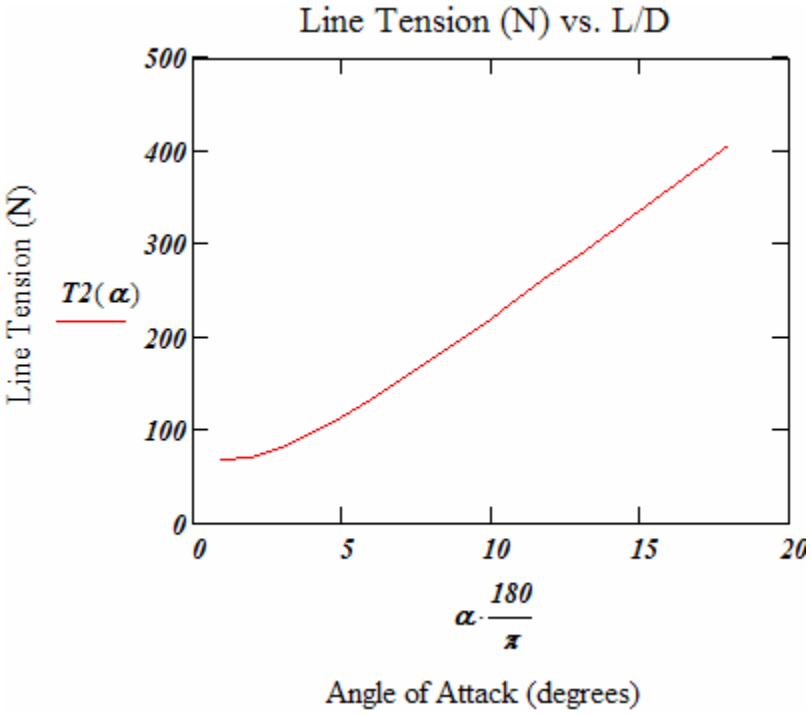

Figure 54 - Kite Line Tension vs. Lift over Drag

From this graph we can estimate that our system will have a line tension force varying anywhere from 75 to 400 Newton's. Now that we have discovered our line tension we can use these values to find the possible chain tension using our pivoting arm model. For the pivoting arm model we used the following values:

W_DA = 28.576 kg	Total Weight of Rotating Arm	W2 = 15.3 kg	Weight of AOA Change
W_BA = 16.329 kg	Weight of Arm from Point A to B	R2 = Ra/2	Distance from Point A to W2
W_DB = 12.247 kg	Weight of Arm from Point D to B	Rc = Ra/2	Chain Distance from Point A
Ra = 2.4348 m	Length from Pivot Popint to A	Rd = 1.829 m	Length from Pivot Point to D

Using equation **(16)** we find the calculated power of the oscillating beam as a function of Angle of Attack:

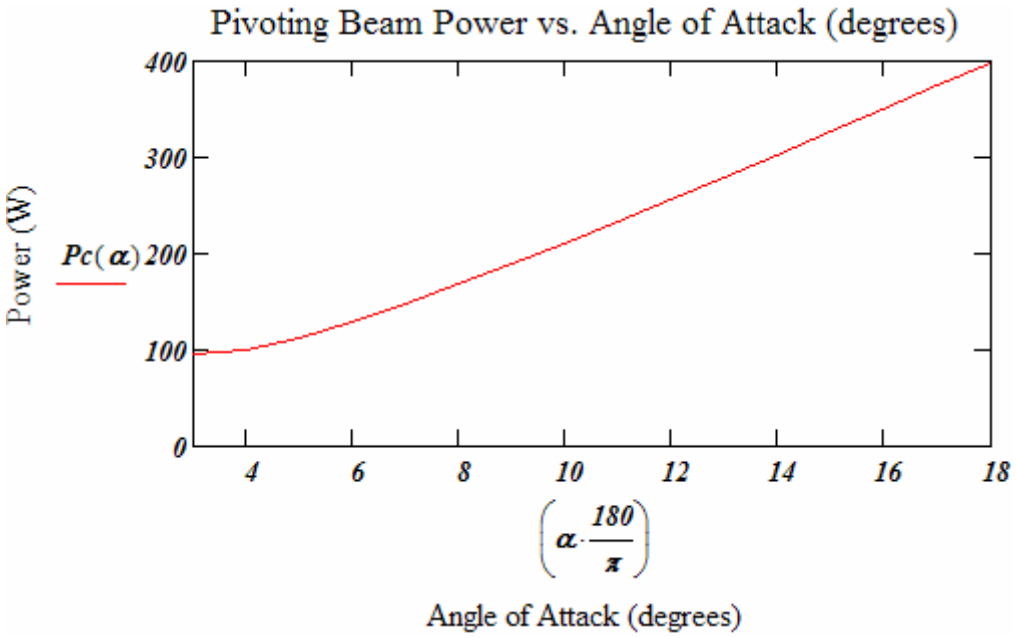

Figure 55 - Pivoting Beam Power vs. Angle of Attack

Using equation **(18)** we find the tension on the chain to vary as a function of Angle of Attack:

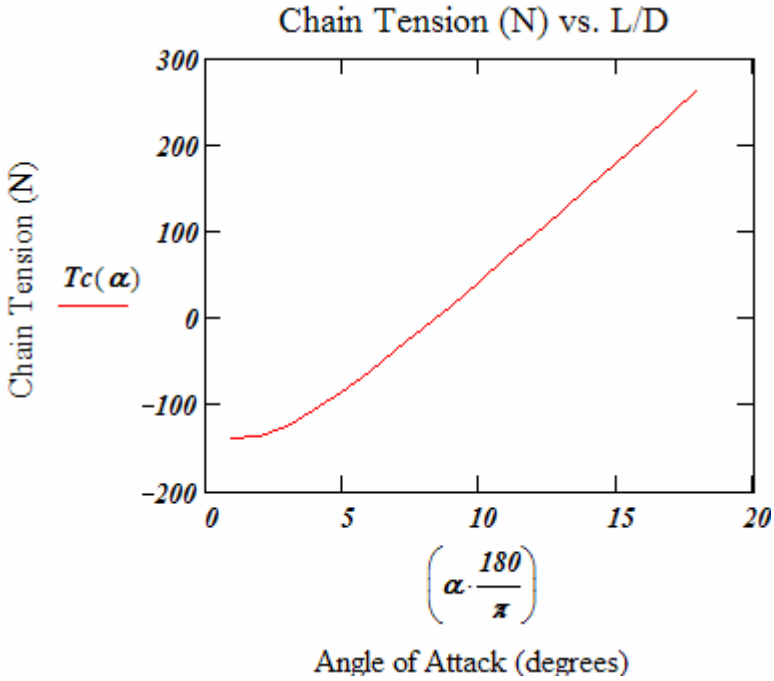

Figure 56 - Chain Tension vs. Lift over Drag

From this graph we can see that estimates show the chain tension to vary from -150 to a possible 200 N of force. The negative values represent that the weight of the pivoting beam arm is still greater than the force of the kite. It can be seen that we can't expect the beam to move until the kite reaches a certain degree for its angle of attack.

Finally, this predicted chain force can then be applied to our gear ratio modeling to determine the possible end torque value for a gear system. For this portion we assume gear that will be used on our gear system. Therefore, our known values are:

r1 = 0.0889	*Gear number one Radius*	*St = 1*	*Stroke Length*
r2 = 0.01905	*Gear number two Radius*	*Sl = 2.4384*	*Stroke Time*
Q1 = 48	*# of teeth on gear one*	*Q3 = 12*	*# of teeth on gear two*

From these values we can determine the final torque on the generator shaft as:

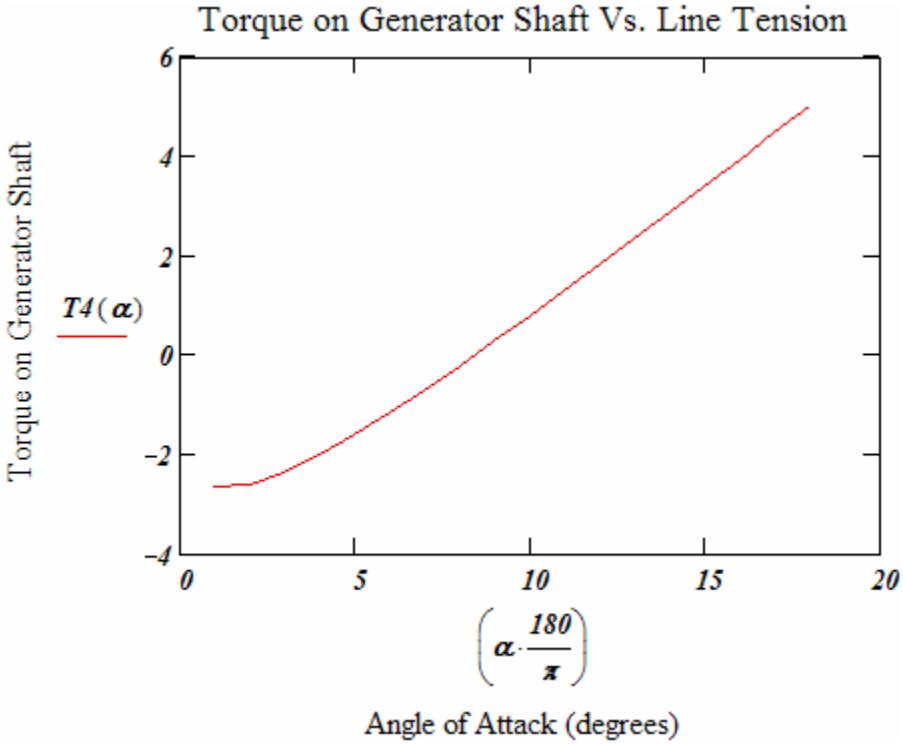

Figure 57 - Torque vs. Lift over Drag

Similar to the Chain tension, the beginning torque is negative when the beam the kite is not moving the beam upward. When the beam finally moves upward we see that the torque on the generator approaches 6 N-m. Using the given values, the possible final RPM on a generator shaft can also be estimated as:

$$RPM2 = 1.048 \times 10^{3}$$

4.2.2 Dynamic Simulation Results

In this section we present results from the dynamic simulations of the kite and rotating arm system. The equations of motion solved in the simulation were summarized in Section 3.3.2.

For the mechanism with the counterweight system, it is ideal to determine what counterweight would produce the highest average coefficient of power for a given wind speed. The Dynamic simulation in the Matlab program can solve for coefficients of power in terms of the counterweights for varying wind speeds. The results for different counterweights and wind speeds runs are presented in Figure 58:

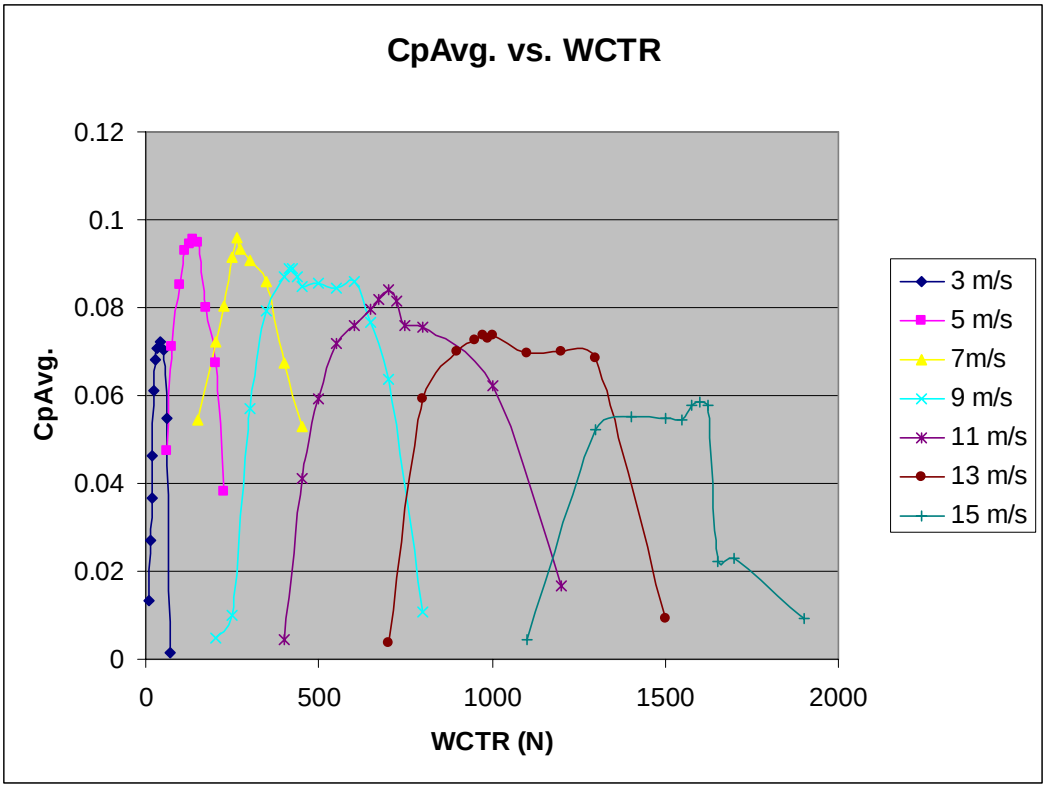

Figure 58 - Average Coefficient of Power vs. Counterweight (N)

From Figure 59, it is apparent that an optimal counterweight exists for each wind velocity. In Figure 59, these optimal WCTR values are presented:

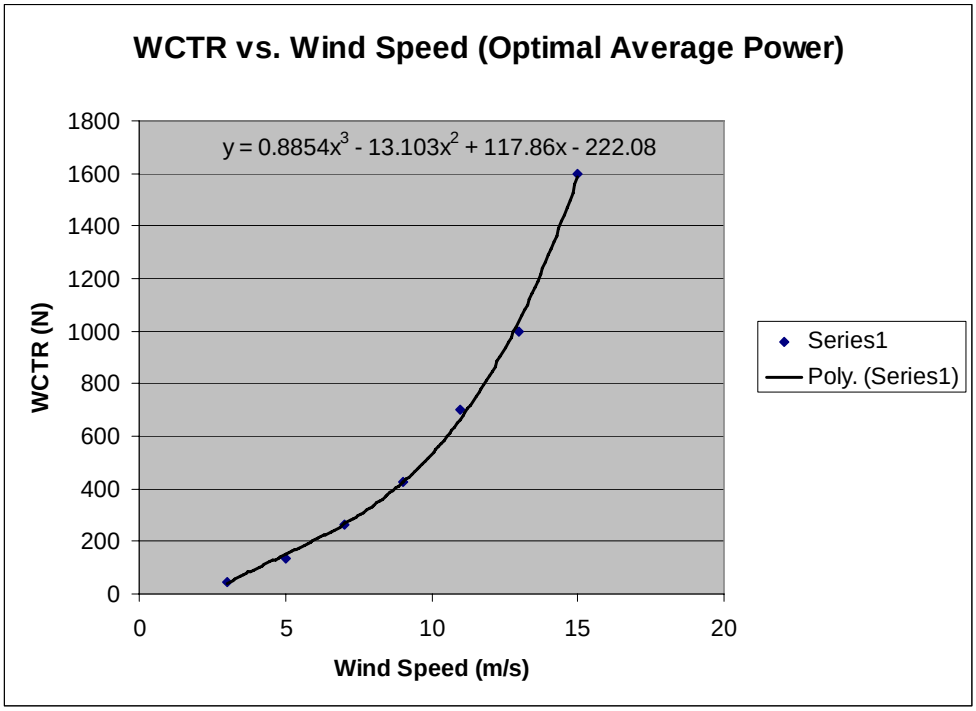

Figure 59 - Counterweight of highest Power Production

Figure 59 could be used during testing of the demonstrator. An operator could reference this chart to adjust the systems counterweight to provide the highest power production for a given wind speed. A curve fit to Figure 59 yields:

$$WCTR = (0.8854)\cdot Vwind^3 - (13.103)\cdot Vwind^2 + (117.86)\cdot Vwind - 222.08 \quad \textbf{(45)}$$

This power coefficient, defined in equation (), is a measure of the fraction of available power available in the wind that is extracted by the mechanism.

$$Cp := \frac{P}{0.5\cdot \rho \cdot A \cdot V^3} \quad \textbf{(46)}$$

In Figure 60, the power coefficient is plotted for the optimal condition.

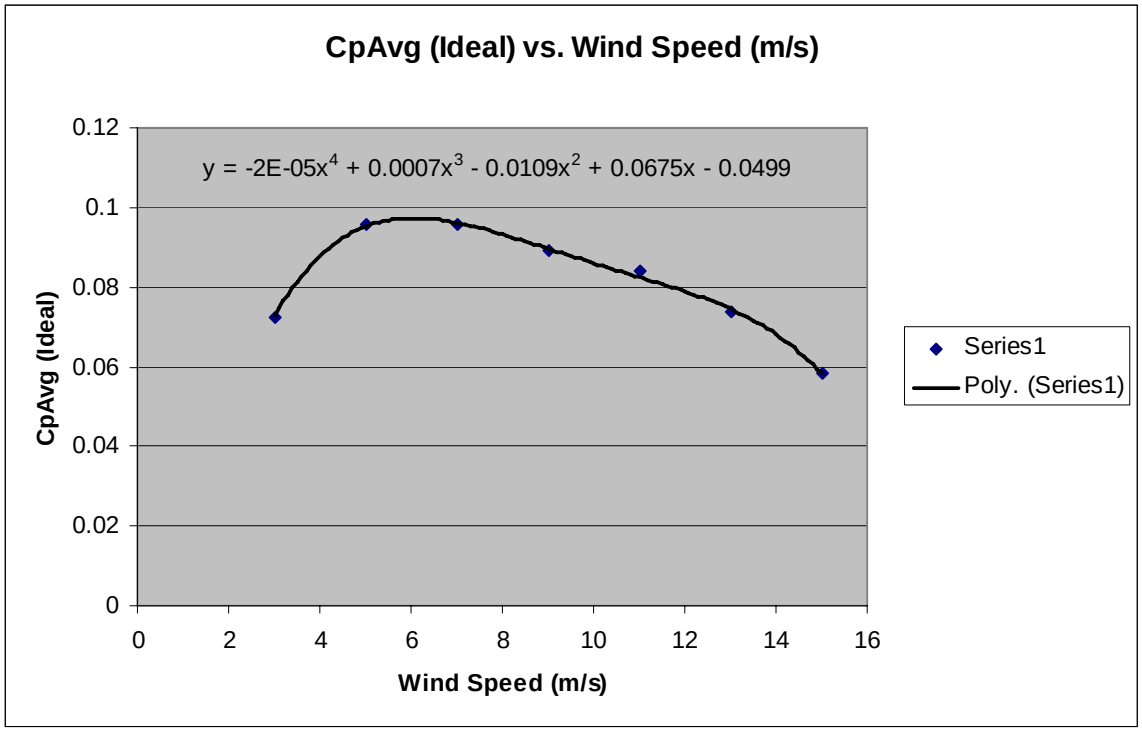

Figure 60 - Highest Coefficients of Power for Wind Speed

From Figure 60, it can be seen that the maximum coefficients of power are reached during wind speeds between five to seven meters per second. This is ideal for the purposes of the project because these wind speeds are the average wind speeds that our kite system will be experience in an area such as Worcester. A curve fit to Figure 60 yields:

$$Cp := \left(-2.5 \cdot 10^{-5}\right) \cdot Vwind^4 + 0.0007 \cdot Vwind^3 - 0.0109 \cdot Vwind^2 + 0.0675 \cdot Vwind - 0.0499$$

(47)

From the average coefficients of power, we can find the optimal power production that the system will generate for a given wind speed. A graph of power produced versus wind speed is given in Figure 61:

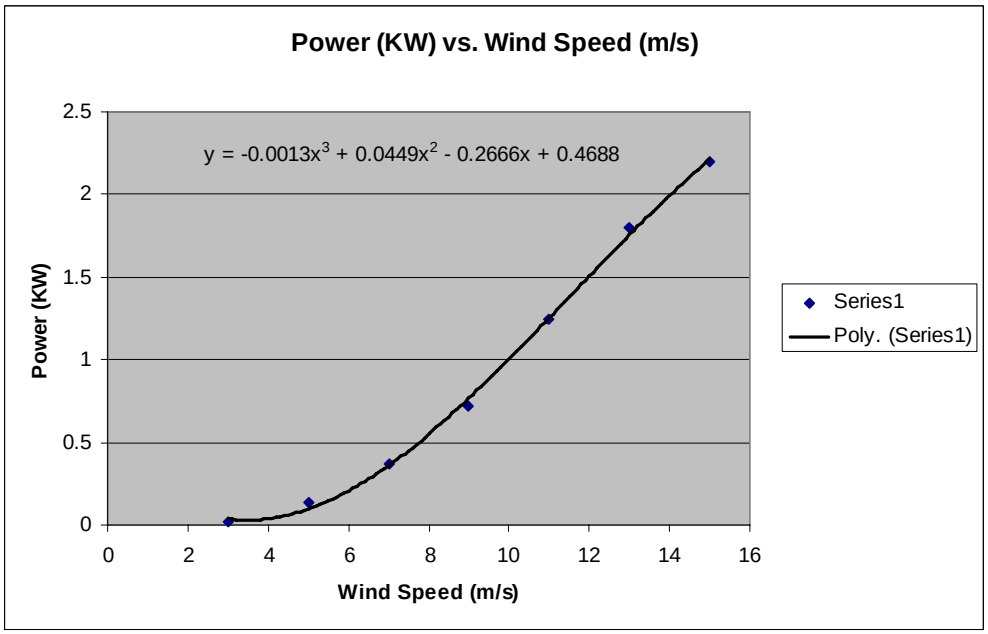

Figure 61 - Optimal Power Production for given wind speed

A curve fit to Figure 61 yields:

$$Power(KW) := (-0.0013) \cdot Vwind^3 + (0.0449) \cdot Vwind^2 - (0.2666) \cdot Vwind + 0.4688$$

(48)

The results of this data show that the kite system will have the ability to produce power approaching the production of similar sized turbine systems. The power Production for our kite system at an average wind speed of 8 m/s is around 0.5 KW. A similar sized turbine at this wind speed and power production would have a rotor diameter of 4.652 meters. For New England areas, such as Worcester, the average wind speed at a high altitude would generate around half a kilowatt.

The average yearly power production for each wind speed is presented in Figure 62. This term is very common in the wind industry and is often used as benchmark of comparison for electrical generating devices.

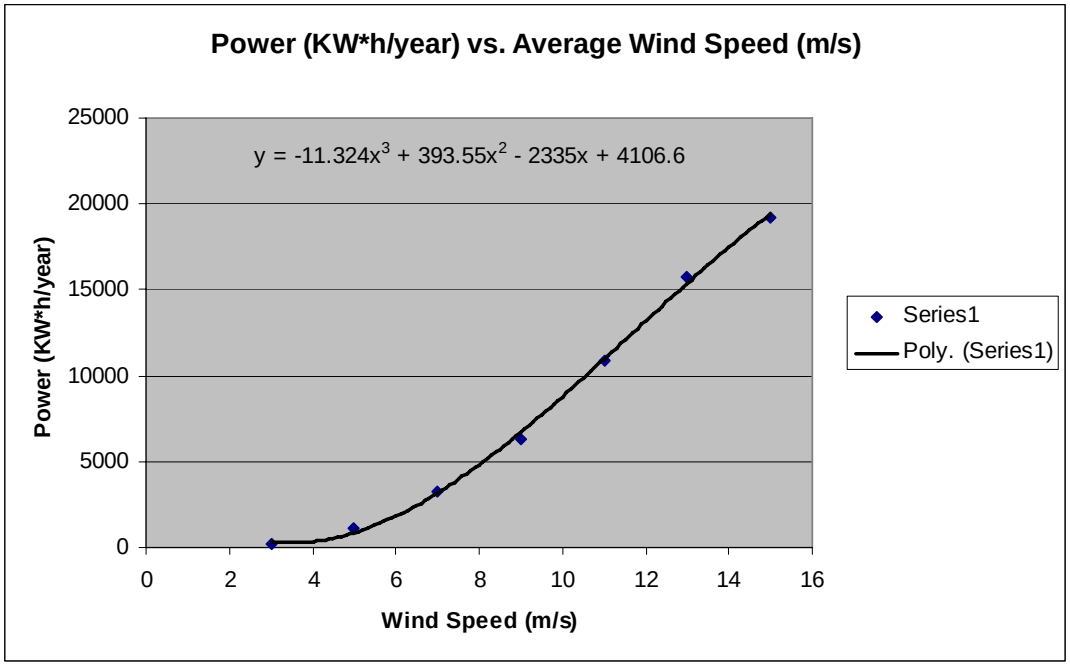

Figure 62 - Yearly power production vs. average wind speed

A curve fit to Figure 62 yields:

$$Power\left(KW \cdot \frac{h}{year}\right) := (-11.324) \cdot Vwind + (393.55) \cdot Vwind^2 - (2335) \cdot Vwind + 4106.6$$

(49)

A further advantage of the dynamic system simulation is the ability to predict the kite's motion. Using the Matlab software we can simulate the path of the kite as it moves through the sky as shown in Figure 63. The wind velocity was assumed to be at 5 m/s, with a counterweight of 135 Newton's set to provide the highest possible average coefficient of power.

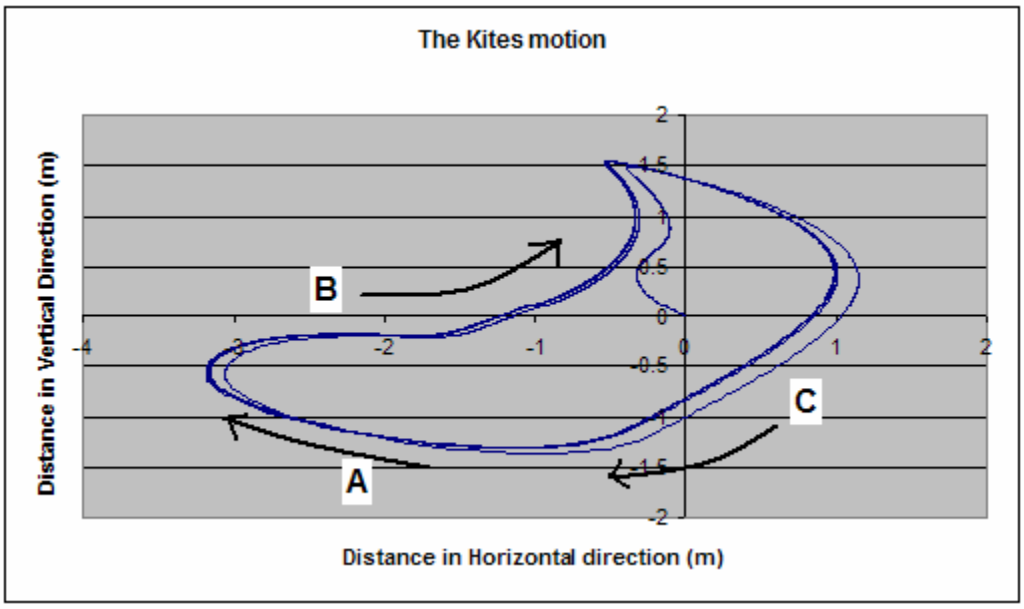

Figure 63 - Kite Motion

The starting point of the kite is at the origin (0,0). Figure () shows that over time, the kite oscillates in a repeating motion. Region A represents when the beam is lowered and the kite's angle of attack has been changed. In this region the growing force of the kite is decelerating the beam. Region B represents the area where the kite and beam are rising upwards. This is the power stroke phase of the system. Region C represents the de-powering of the kite combined with the oscillating beam falling downward.

In Figure 64 the oscillating motion of the beam is presented. The angle of the beam over time is shown as:

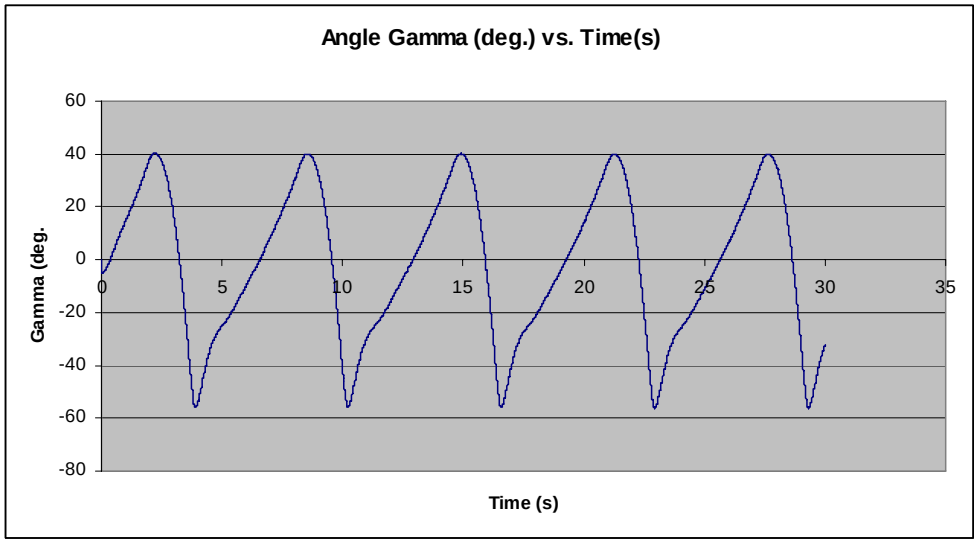

Figure 64 - Simulated Angle gamma (deg.) vs. Time (s)

The oscillation of the beam appears to oscillate between:

$$-60 \leq \theta \leq 40$$

When θ = 0, the oscillating beam is the horizontal. At θ = 40 is the beam is 40 degrees above the horizontal plane and at θ = -60 the beam is 60 degrees below the horizontal plane. The oscillation in the oscillating beam corresponds to the change in the kite's angle of attack. When the Gamma angle is at -60 degrees the kite's angle of attack reaches a maximum, where it then pulls the beam upwards increasing the beam's Gamma angle. As the Gamma angle increases, the kite's angle of attack decreases slowly once theta is greater than the horizontal. Eventually at 40 degrees the Kites angle of attack has reached zero and when of the beam pulls it back down where the process repeats.

We can also determine the varying line tension caused by the kite's motion:

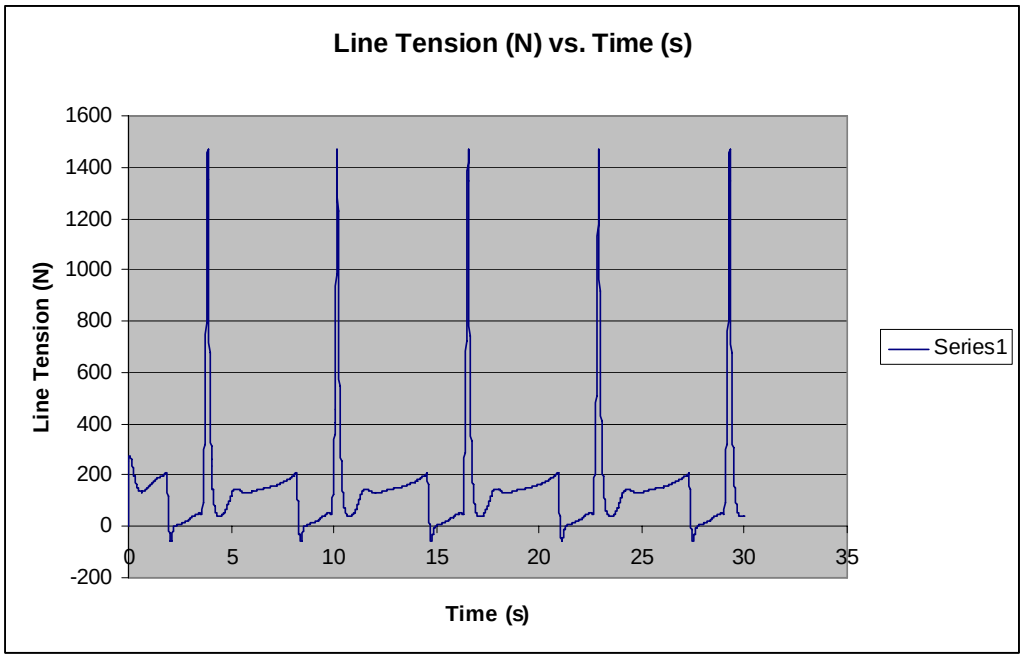

Figure 65 - Simulated Line Tension (N) vs. Time (s)

In Figure 65 it is interesting to note the periodic large amplitude peaks. These high peaks occur when the kite suddenly changes its angle of attack as the rotary beam moves downward in the descent phase. The large amplitude line tension serves to decelerate the rotary beam as it descends. These large line tensions could fracture the kite tethers if the line tension exceeds the tether tensile strength. We estimate the tensile strength of each of the kite line at 2648 Newton's. We estimate the majority of the line tension to reside on two kite lines, yielding a margin of safety around 3.5. It is also important to realize that the dynamic simulation alters the Angle of Attack between the ascent and descent stages over a 0.25 second time interval. If the time is larger in the actual operation of the demonstrator, these peak line tensions may be reduced.

In Figure 66, the Lift over Drag predictions from the added aerodynamic analysis are presented:

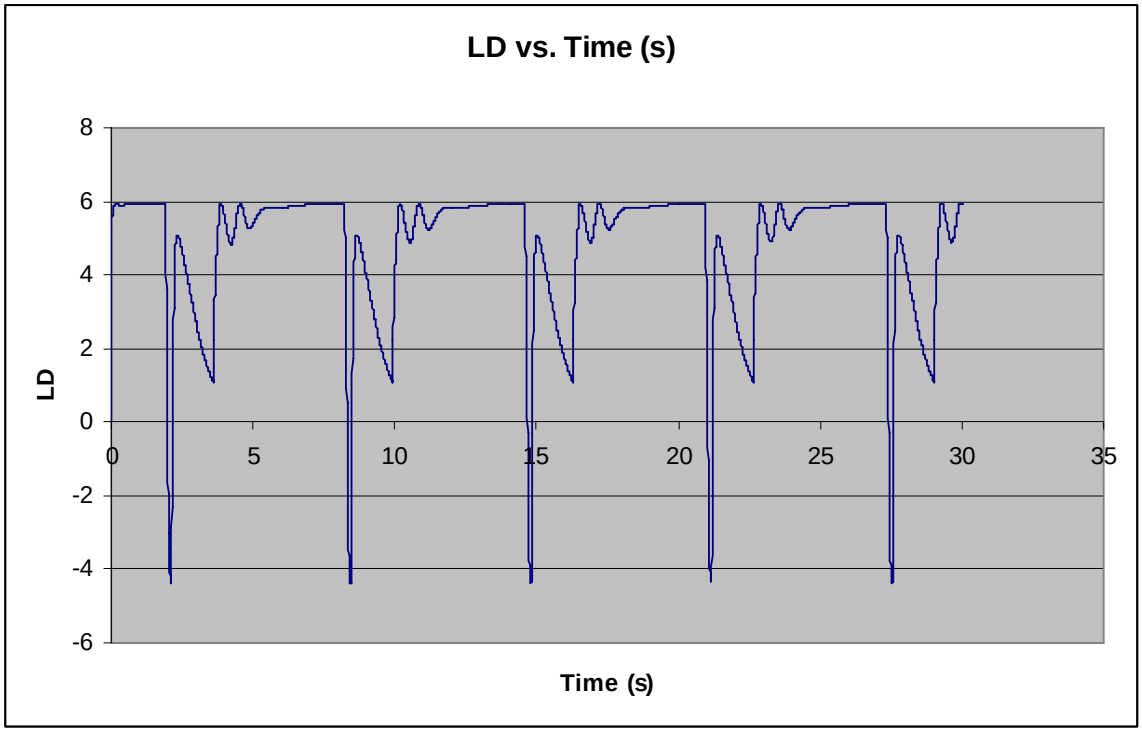

Figure 66 - Simulated Lift over Drag vs. Time (s)

The downward large amplitude peaks in the lift over drag ratio are a result of the high peaks in the line tension. The maximum L/D values are around 6 when the kite and beam are moving during the ascent phase. The minimum L/D varies between one and four during the descent stages of the kite's motion. These L/D values reasonably approximate the L/D values set by Goela (1986).

In **Figure 67**, the values of the coefficients of lift versus the coefficients of drag are presented:

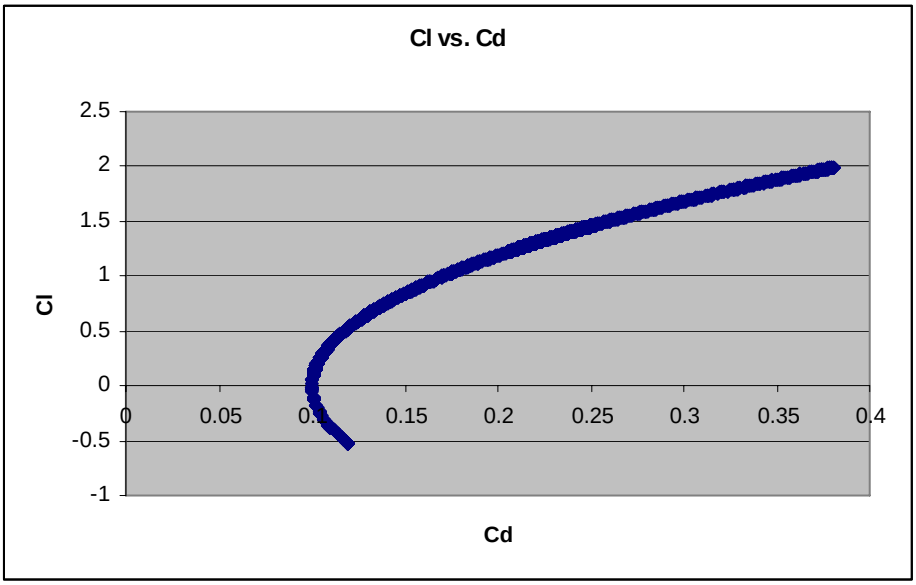

Figure 67 - Simulated Cl vs. Cd

4.3 System Stress Analysis

Stress calculations for the Sprag Combo begin with the analysis of the long pivoting beam. The concern is whether the beam can withstand the full force of the kite pulling on one end of the beam. The stress calculations for the beam are based on the equations found in Section 3.4. For the aluminum beam being used in the system the cross section lengths of the beam and the calculated moments of inertia and section modulus are:

$$A = 3.5in \qquad I = 1.693in^4$$

$$B = 3.375in \qquad Z = 0.967in^3$$

For the stress calculations a beam length of approximately 7 feet was assumed, while the kite force was approximated from our calculations in the system simulation section. Using this variable kite tension from steady state analysis, the shear stress on the beam as it moves upwards can be determined. The final calculations show:

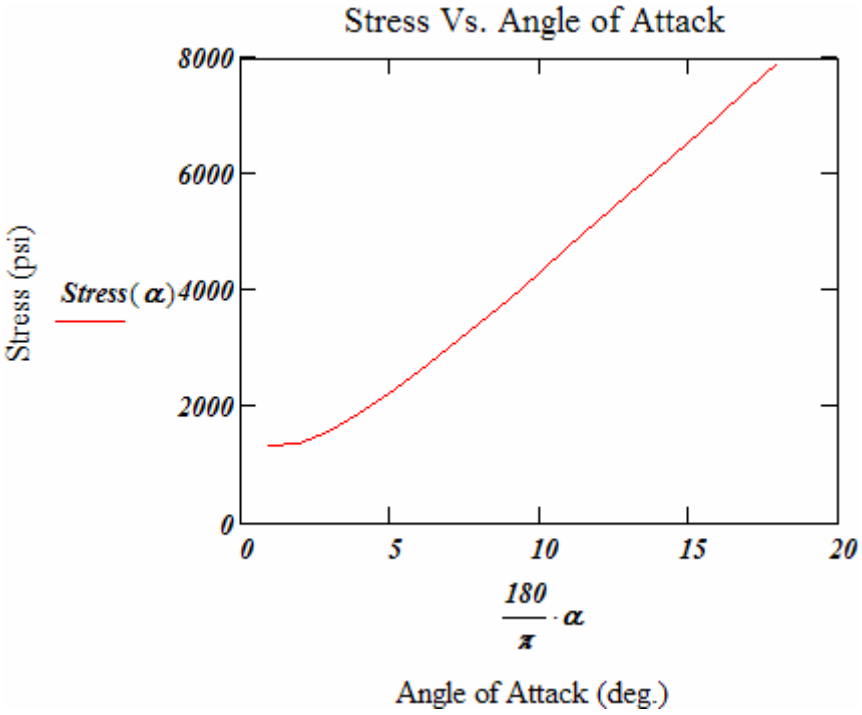

Figure 68 - Stress vs. AOA

The calculations show that the beam stress will vary between from 1-8(Ksi), which is well below the yield strength of aluminum (32 Ksi). The other concern with the beam is its deflection. The beam material is Aluminum 6063, with an Elasticity module of:

$$E = 70GPa \quad \text{or} \quad E = 10150ksi$$

Using equation **(40)** and kite forces from steady state, Figure 69 shows the Beam Deflection vs. Angle of Attack.

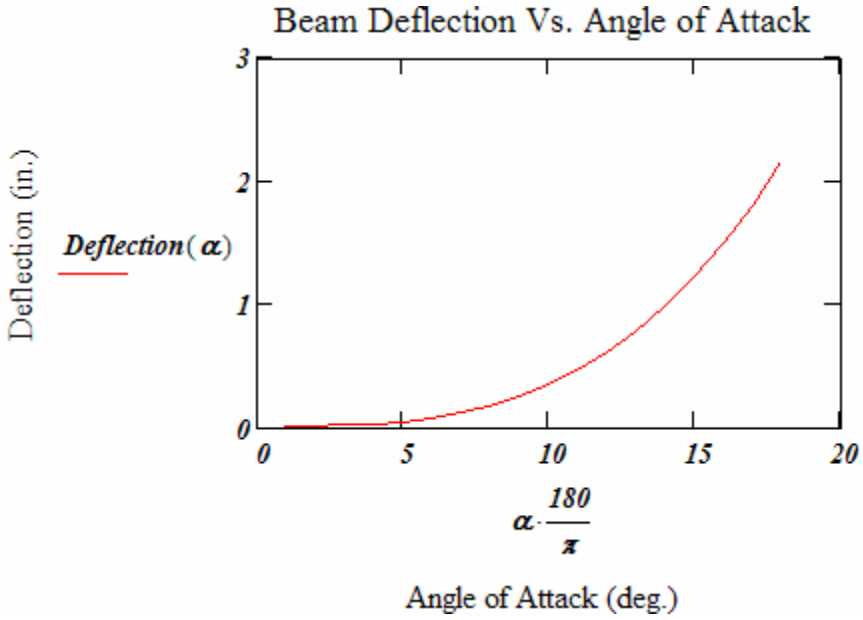

Figure 69 - Deflection vs. AOA

Calculations for the beam deflection show that the beam will deflect from 0-3 inches over the course of the kite's ascent.

The next questionable portion of the system is the center beam on which the pivot rests. The beam in this case is a 4x4 cross section of wood. Wood is considered to have an Elasticity module of approximately 10MPa. The Moment of Inertia and section modulus for the beam is calculated to be:

$$I = 85.32in \quad Z := 21.33in$$

The load placed at the pivot point is effectively equal to the moment created on the support beam of created by the conjunction of the oscillating arm and the kite force. Using the moments created by the oscillating beam, the stress on the center beam is found to vary from 1-4ksi. Well within the yield strength of wood.

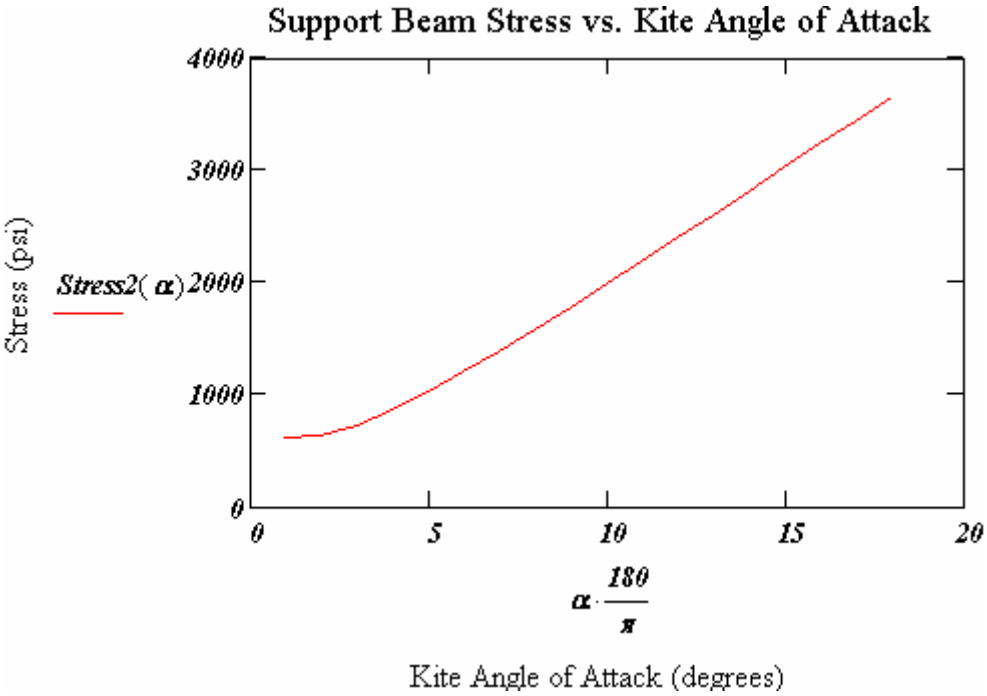

Figure 70 - Support Beam vs. Kite Angle of Attack

The maximum deflection of the support beam is at the center of the beam near the pivot of the oscillating beam. Using equation **(42)**, the deflection is:

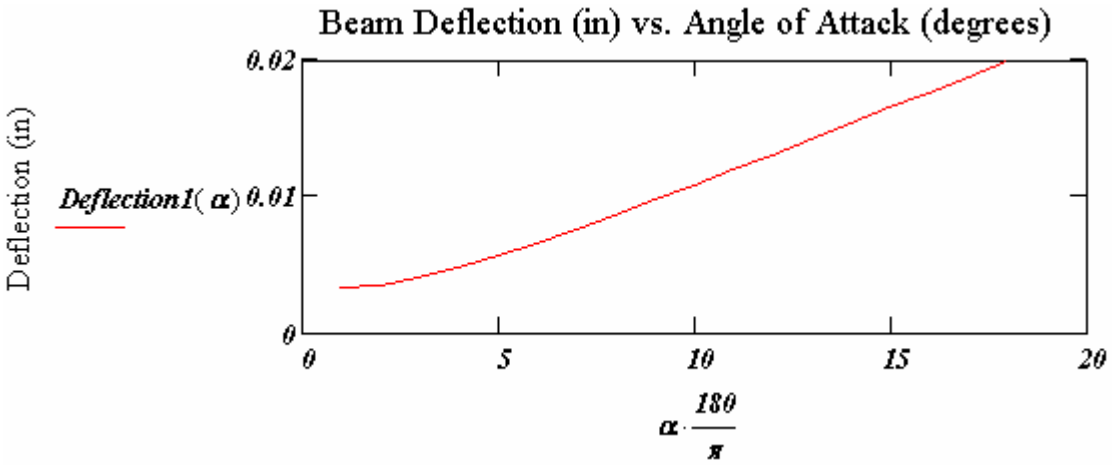

Figure 71 - Beam Deflection vs. Angle of Attack

From Figure 71, the beam deflection on the central support beam is minimal.

5. Conclusions

To begin the process of designing the kite power demonstrator different types of kites were researched until a final decision could be made as to the ideal kite for a demonstrator. The chosen kite is any one of a series of production kite boarding kites known as twinskin kites manufactured by Peter Lynn. The main benefit of these kites was the auto-zenith feature that enabled the kite to remain stable in the air with minimal user input.

Two different testing setups were completed in the overall kite testing portion of this project. Preliminary testing of kite boarding kites was done with several different kites with the goal of measuring potential line tensions, though none of these kites were a twinskin model. After the purchase of the Peter Lynn Guerilla twinskin kite-boarding kite, testing proceeded to determine potential line tensions to determine kite lifts and other key kite dynamic characteristics for simulation purposes.

The second portion of the project was to design and build the kite power demonstrator to be used in concert with the Peter Lynn Guerilla. Several different mechanism concepts were considered until an evaluation matrix was used to determine the best option for the demonstrator. After the decision for the basic design was made, design modifications and optimizations were made in order to simplify the system until the design iterations led to the final design presented in this project report. Construction commenced with the completion of the system design. The current stage of construction is discussed in section 3.2.4. At this stage, the construction to be completed pertains to the retraction spring which will need some future work before completion.

Tying together the two main aspects of the project, the kite and the mechanism, are the various simulations completed. Simulations began with simple steady-state analysis of a generic kite moving at constant velocity with the purpose of analyzing the kite dynamics of the kite itself. Dynamic simulations were introduced to couple the kite dynamics with the specific geometries and characteristics of the balanced beam kite power demonstrator design. The dynamic modeling was used to determine the potential performance, with respect to power output, of the kite power demonstrator in conjunction with the kite.

In order to prove the concept addressed in this project, some preliminary testing will be completed in early May 2007. Since the construction of the retraction mechanism has yet to be completed, a simple counterweight will be utilized to aid the angle of attack change mechanism in bringing the balanced beam back to the starting position. The use of the counterweight is merely a simplification of the retraction spring concept that will be required in future work in order to apply a variable force to the kite in its down stroke as well as to engage the gear and axle assembly to generate the electrical energy.

5.1 Future Recommendations

- Refine AOA Mechanism
    - The design of the preliminary angle of attack change mechanism has been completed, but testing has yet to be done on the constructed mechanism. Work may be required to determine the appropriate weight to be incorporated into the system.

- Refine Retraction Spring Mechanism
    - A preliminary design for the retraction mechanism has been completed, but due to time constraints the system was not constructed. Though the design was completed there are several issues that could be addressed. First of all it will be necessary to find some form of a spring mechanism that will extend to the required length. Second, if the current design is taken then the custom 'chain pulley' will have to be modeled and milled.

- Refine Roll Control Mechanism
    - The system consisting of springs for the roll control mechanism has been considered, but little work has been accomplished in the final design of a system to control the potential roll of the kite in motion. More intensive work should be done in order to determine if a system will be required and what components this system could consist of.

- Finish System Construction – Sprag Clutch
    - Due to budget constraints the sprag clutch, which is meant to stop the gear system from turning when the kite is in its down stroke, was not purchased and attached to the system. With future budgets a sprag clutch should be

purchased and attached to the large sprocket in the gear system. A sprag clutch would typically be welded to the side of the gear and tightened on the axle with set screws.

- Research Different Line Setups
  - For this project a standard line setup was adopted to keep the setup as simple as possible for initial testing. Future testing may incorporate different line setups to test kite performance. Different setups may be switching the leading and trailing edge lines or simply trimming the kite lines to optimize performance.

- Test Potential Energy Output of Fully Constructed System
  - Once the system is fully designed and constructed, a torque meter should be used to determine the resultant torque on the axle holding the small sprocket. This test setup will further prove that a kite power demonstrator has power output capabilities similar to that of a small wind turbine.

- Extended Testing on Kite Dynamics
  - Due to time constraints physical testing of the kite was limited and thus this portion of the project should be expanded upon in the future. More in depth analysis of kite dynamics may bring forth significant changes in the system design when considering the effects of wind gusts and changing wind direction.

- Long-term Analysis of Weathering on Kite
  - One major concern with a kite-powered system is the effect that weather may have on the rip-stop nylon material of the kite over extended periods

of time. Such concerns that should be considered are UV degradation, lightning strike sustainability, and ability to withstand extended periods of rain and sleet.

- Increased Altitude
  - When the concept was first developed in the late 1970's it was intended for altitudes approaching 5000 feet. Due to FAA restrictions, a kite in the U.S. cannot exceed 150 feet in altitude without modifications. We have yet to test the system and kite together, but aim to test the kite at an altitude of 80+ feet. In the future it may be beneficial to test the kite at an altitude approaching the 150' mark or even higher with the required modifications.

- Extended Use of System
  - Initial testing of the system will primarily consist of launching the kite attached to the system and testing it for a short period of time, a number of minutes. In the future the system should be optimized so as to launch and fly for an extended period of time, possibly several hours or even a day.

References:

1. Goela, J. S. "Wind Power Through Kites." Mechanical Engineering 42 (1979): 42-43.

2. Goela, J. S., R. Vijaykumar, and R. H. Zimmermann. "Performance Characteristics of a Kite-Powered Pump." Journal of Energy Resources Technology 108 (1986): 188-193.

3. Goela, J.S. "Wind Energy Conversion Through Kites." January 1983. Indian Institute of Technology Kanpur

4. Goela, J.S., Varma, Sanjeev K. "Effect of Wind Loading on the Design of a Kite Tether." Journal of Energy. Vol. 6 No.5 1982

5. Loyd, Miles L. "Crosswind Kite Power." Journal of Energy. Vol. 4 No.3 May-June 1980.

6. Nicolaides, John D., Speelman, Ralph J., Menard, George L. C. "A Review of Para-Foil Applications." Journal of Aircraft. Vol.7 No.5 Sept.-Oct. 1970.

7. Vijaykumar, R. Performance Characteristics of a Kite-Powered Pump. M. Tech. Thesis, Department of Mechanical Engineering, IIT Kanpur, Apr. 1984.

8. The Drachen Foundation. 2006. 09 Oct.-Nov. 2006. <http://www.drachen.org>.

9. Lynn, Peter. Peter Lynn Kiteboarding. 2006. Oct-Nov. 2006. <http://www.peterlynnkiteboarding.com>.

10. "Wind Turbines." April 2007. <http://www.rpc.com.au/products/windturbines/wind_faq.html>

11. "Kite Wind Generator." 2006. April 2007. <http://www.sequoiaonline.com/blogs/htm/progetto_eng.htm>

12. "Kite –Tugs." 2003. April 2007. <http://foxxaero.homestead.com/indsail_028.html>

13. Lang, David. "Electrical Power Generation Using Kites." Drachen Foundation. December 2005

APPENDIX A: Drachen Foundation

The Drachen Foundation is a non-profit organization dedicated to educating the public about the history and science of kites. In addition to funding classroom activities and public events, they also do research into using kites for other means, such as power generation. The decision matrix used to evaluate our initial concept mechanisms was based on a similar matrix used in a 2005 paper to compare and contrast the feasibility of various kite-based power generation concepts.

APPENDIX B: Heifer International's Overlook Farm

Heifer International is a non-profit organization dedicated to educating the public on poverty and living conditions in under-developed nations. Additionally Heifer seeks to train people to be self-sufficient and put an end to poverty and hunger around the world through knowledge and understanding. Overlook Farm is a 270-acre working farm in Rutland, MA that is open to the public to demonstrate poverty solutions. This site is the designated test site for the kite power demonstrator, chosen for its proximity to the WPI campus and its relatively high elevation. Additionally, Overlook Farm resides in a class 3 wind zone, meaning on average the wind speed is 6.5 to 7 meters per second, or 14.5 to 15.7 mph.